6-25-2010

# Spatial spread of infectious diseases

Aaron Mora

Aaron Mora
*Candidate*

Mathematics
*Department*

This thesis is approved, and it is acceptable in quality and form for publication:

*Approved by the Thesis Committee:*

Peter J Embrechts, Chairperson

# Spatial Spread of Infectious Diseases

by

**Aaron Mora**

B.S., Applied Mathematics, University of New Mexico

THESIS

Submitted in Partial Fulfillment of the
Requirements for the Degree of

Master of Science
Mathematics

The University of New Mexico

Albuquerque, New Mexico

May, 2010

# Dedication

*To my parents, Toni and Ray, for their support and encouragement.*

# Acknowledgments

I would like to recognize and acknowledge Professor Pedro Embid for his dedication to the the completion of this paper. Without his guidance this would not have been possible. He has been a tremendous teacher, adviser and mentor and I am forever grateful. Gracias por toda su ayuda.

I would also like to thank Professor Eric Toolson and Professor Helen Wearing for taking the the time to be a part of my committee.

# Spatial Spread of Infectious Diseases

by

**Aaron Mora**

ABSTRACT OF THESIS

Submitted in Partial Fulfillment of the
Requirements for the Degree of

Master of Science
Mathematics

The University of New Mexico

Albuquerque, New Mexico

May, 2010

# Spatial Spread of Infectious Diseases

by

**Aaron Mora**

B.S., Applied Mathematics, University of New Mexico
M.S., Mathematics, University of New Mexico, 2010

## Abstract

In this thesis we do a comparative study of diffusive models with non-diffusive models, looking at the effect movements in the form of diffusion, have on the spreading of infective diseases. This study is undertaken within the context of the SI and SIR models, two of the most fundamental models for the propagation of infectious diseases. The diffusive SI and SIR models are supplemented with no flux boundary conditions to insure meaningful comparison of the populations predictions. In addition, we use a one dimensional spatial domain for computational simplicity. The comparison of the SI (and SIR) model with its diffusive counterpart is carried out for a broad spectrum of diffusivities. We identify their ranges of diffusivities for which the predictions of the diffusive and non-diffusive model are in agreement. Interestingly, we discovered that in the subcritical case, the diffusive SIR model predicts an epidemic outbreak whereas the standard SIR model does not.

# Contents

# List of Figures

# Chapter 1

# Introduction

In this thesis we undertake a mathematical study of two of the most fundamental models for the development and the spread of infectious diseases and the outbreak of epidemics. These models include the SI model and the SI model with diffusion and the SIR model and the SIR model with diffusion. These models get their name from the individuals that make up the population in which said epidemic is taking place, that is, these individuals are broken down into three types of individuals: Susceptible ($S$), Infected ($I$), and Recovered ($R$) with the last individual obviously not appearing in the SI model. The defining difference between the models without and with diffusion is the capability of individuals in the latter models to move in space which we will limit to one space dimension and no flux boundary conditions to insure proper comparison of the population predictions of the diffusive versus the non-diffusive model. Because of the simplifying assumption always present in the formulation of mathematical models, the epidemics that develop within these models, do so in a controlled environment, with specific restrictions dictating their behavior. In particular, we do not account for birth and death rates and other natural occurrences. In spite of these simplifications, these models are basic for understanding the propagation of epidemics in space and their growth in time.

We begin in Chapter 2 with the SI model and the famous Kermack-McKendrick model, also known as the SIR model. We do a thorough analysis of both models beginning with the simpler SI model and then moving onto the more difficult SIR model. In context with the SI model, the SIR model admits a critical parameter (called $c$) so that only for non-dimensional initial data about $c$ there is an epidemic outbreak. We first detail how each model is derived and then look at a criterion for the development of an epidemic in each model. When possible we provide detailed analytical solution for these models and otherwise we produce accurate numerical solutions to explain their qualitative behavior.

In Chapter 3 we look at the SI model with diffusion. First we construct the diffusive SI model by adding Fickian (Fourier) diffusion to both the infected and susceptible populations. After discussing a few basic properties of the solutions we proceed to a detailed numerical study of the solutions over a wide range of diffusivities for the infected and susceptible populations. These numerical solutions permit a quantitative comparison of the predictions of the SI versus the diffusive SI model and to assess when their predictions are close or disparate.

In Chapter 4 we carry out a similar analysis for the diffusive SIR model. Unlike the former SI model with diffusion, we have additional effects from the recovered individuals. Once more we study the numerical solutions for a broad range of diffusivities for the susceptible, infected and recovered populations and under subcritical and supercritical initial conditions. Because of the potentially enormous number of numerical experiments involved, we make the simplifying, yet reasonable assumption that diffusivities of the susceptible and the recovered are the same. Again, the predictions of the SIR and the diffusive SIR model are close or not. Also, very interestingly from the qualitative and quantitative sides is the discovery that for the subcritical case, the diffusive SIR model predicts an epidemic outbreak but the standard SIR model does not.

Finally, in Chapter 5 we end with a summary and the most significant conclusions in this thesis.

# Chapter 2

# Mathematical Modeling of Infectious Disease

## 2.1 Introduction

Throughout history the spreading of infectious diseases has had devastating effects on humans as well as animal populations. In some cases the rapid spread of infectious diseases result in epidemics or even pandemics, and they are responsible for the deaths of millions of people over vast areas of the earth. Examples of such infectious diseases include the European Plague or Black Death, small pox, influenza, HIV/AIDS, avian flu, and the swine flu. Possibly the earliest and most catastrophic epidemic ever recorded was the Black Death of the 14th century which resulted in the estimated deaths of one third of a population of Europe, at the time about eighty five million people. To put this into perspective, it caused more deaths than those in World War I and II combined. The plague was transmitted by the fleas of black rats to humans and then to other humans. The plague flourished because it developed in an environment that had extremely poor and unsanitary living conditions and also

because most individuals believed that the epidemic was attributed to evil spirits or a vengeful God, and therefore many thought that prayer alone would save them. Consequently, their lack of a fundamental understanding as to how infectious diseases are transmitted led to the massive number of deaths seen. Of course this was not the only deadly epidemic observed. One would be remiss not to also mention the whole host of infectious diseases, influenza and smallpox just to name a few, unleashed on unsuspecting native inhabitants during the conquest of the so called "New World", who were not previously exposed to these diseases, which resulted in the deaths of millions of native americans. These diseases where spread by human contact, most notably by coughing and sneezing near one another, or through physical contact, i.e. a handshake from a person who had previously sneezed into their hands thereby transferring the infection. It goes without saying that smallpox and influenza are not limited to this particular region, it is also linked to millions of deaths around the world at differing points in time. Moving onto a more recent infectious disease, HIV/AIDS, has also led to millions of deaths throughout the world, with the largest concentration of deaths being in Africa. Now, HIV/AIDS, is different in that the human contact previously mentioned does not apply to how this disease is spread. It is a sexually transmitted disease which means that the dynamics of its transmission is different. Fortunately, advancements in medicine, technology, and in an overall awareness of disease transmission, has meant that we have drastically cut down on the number of potential deaths caused by infections. This is made evident by the avian flu and swine flu pandemic, which at the time of this paper being written were the most conspicuous diseases. Our current knowledge of the transmission, prevention and treatment of infectious diseases has aided in stopping these diseases from turning into full blown epidemics and as we know, leading to loss of human life on a large scale. Epidemiological studies have produced several models and explanations as to how epidemics occur and spread, with the objective of the studies being to prevent or limit the impact of epidemics. As far back as 1760, the mathematician

Daniel Bernoulli introduced one of the first mathematical models, which looked at the spread of small pox [4]. After a long hiatus of more than 150 years, Kermack and McKendrick did ground-breaking work in the mathematical analysis of the spread of infectious diseases. In a series of papers [14] they introduced the so called SIR model to study the plague epidemic that swept over Bombay in 1905-1906. An important contribution in their work was the introduction of critical conditions to trigger the epidemic. Work on the mathematical modeling of epidemics has continued ever since and the 1980's witnessed an explosion of activity in this area due partly to our increased understanding of dynamical systems and Partial Differential Equations, together with advances in numerical computing and simulations. Examples of research in the mathematical modeling of epidemics include the work of Heathcote and Yorke [8] on the transmission of gonorrhea, Noble [23] and Raggett [24] on the spread of the plague, Anderson et. al. [3] on the transmission dynamics of HIV and Anderson et. al [1], K*á*llen et. al. [12], MacDonald [18], and Murray et. al. [21] on the spread and control of rabies. The work in this field has expanded to a great extent and comprehensive accounts have appeared in the influential works of Murray [19] [20], the textbook of Edelstein-Keshet [5] and the monographs of Fife [6], Hoppensteadt [10], [11], and MacDonald [18]

In this chapter we will look at the two most basic models for the transmission of infectious diseases, namely the SI and SIR models. We study these models in order to gain insight into the mechanisms that bring about the spread of infectious diseases. These models have been helpful to describe how certain infectious diseases, those mentioned beforehand, such as the Plague, HIV, AIDS, influenza and small pox, spread as time progresses. The SIR model was introduced by Kermack and McKendrick [14] in their seminal study on the transmission of the plague in the Bombay epidemic of 1905-1906. Both the SIR model and the SI model are examples of what is known as compartment models [5], [6], [19]. Specifically, the population of individuals is separated into three class: the susceptible ($S$) who can contract

the disease, the infected ($I$) who have contracted the disease and can spread it, and the recovered or removed ($R$) who are either immune to the disease or isolated until recovered. The main difference between the SIR and the SI model is that the latter does not include the class of recovered individuals. In the remaining two sections of this chapter we will describe the main features of the SI and the SIR models.

## 2.2 SI Model

Let us begin by describing how the SI model is constructed. We start with the following assumption: The total population of individuals is divided into two classes, the infected individuals ($I$) and the non-infected, but susceptible individuals ($S$). At time $t$ their respective amounts are $S(t)$ and $I(t)$. Now with $S(t)$ and $I(t)$ representing the susceptible and infected classes respectively within the population, and the total population which we will call $N(t)$, is given as $N(t) = S(t) + I(t)$, we assume the following:

1. The basic mechanism of infections involves the interaction (by proximity) of the infected ($I$) and the susceptible ($S$), where we assume an interaction reaction akin to a chemical reaction of the type

$$S + I \xrightarrow{a} I$$

and with a growth rate of $I$ governed by the law of mass action, so that the increase of the infective class is at a rate proportional to the number of infected and susceptible, i.e. given by $aSI$ where $a > 0$ is a constant parameter.

2. No other birth or death mechanism is assumed in the model (e.g. Malthusian or logistic growth for $S$)

Using both of the assumptions stated above, we get the SI model for the propa-

gation of an infectious disease

$$\begin{aligned} \frac{dS}{dt} &= -aSI \\ \frac{dI}{dt} &= aSI \end{aligned} \tag{2.2.1}$$

with initial conditions

$$S(0) = S_0 \geq 0 \quad \text{and} \quad I(0) = I_0 \geq 0. \tag{2.2.2}$$

The fixed population is built into the model, so that when adding up the equations in the system we obtain,

$$\frac{dN}{dt} = \frac{dS}{dt} + \frac{dI}{dt} = -aSI + aSI = 0 \tag{2.2.3}$$

so that

$$N(t) \equiv N(0) = N_0 = S_0 + I_0 \tag{2.2.4}$$

where $N_0$ is a constant that represents the total population size. This is known as a conserved quantity.

Now, this system of equations can be simplified, through non-dimensionalization whereby we chose appropriate scales for the variable $I$, $S$, and $t$. Specifically, we introduce the non-dimensional variables

$$\widetilde{I} = \frac{I}{N_0}, \qquad \widetilde{S} = \frac{S}{N_0}, \qquad \widetilde{t} = a(N_0)t \tag{2.2.5}$$

where $N_0 = S_0 + I_0$, and for the total population of this system, which we will label as $\widetilde{N_0}$, we have

$$\widetilde{N_0} = \frac{S_0}{N_0} + \frac{I_0}{N_0} = \widetilde{S_0} + \widetilde{I_0} = 1. \tag{2.2.6}$$

Now if we plug in these equations into Eq.(2.2.1) we have

$$\begin{aligned} a(N_0)^2 \frac{d\widetilde{S}}{d\widetilde{t}} &= -a(N_0)^2 \widetilde{S}\widetilde{I} \\ a(N_0)^2 \frac{d\widetilde{I}}{d\widetilde{t}} &= a(N_0)^2 \widetilde{S}\widetilde{I}. \end{aligned} \tag{2.2.7}$$

Dividing each equation in the above system by $a(N_0)^2$, and for simplicity dropping the new tilde notation, we arrive at the non-dimensionalized SI model which is

$$\begin{aligned} \frac{dS}{dt} &= -SI \\ \frac{dI}{dt} &= SI \end{aligned} \tag{2.2.8}$$

with initial conditions

$$S(0) = S_0 \geq 0 \quad \text{and} \quad I(0) = I_0 \geq 0. \tag{2.2.9}$$

and the total population being

$$N(t) \equiv N_0 = S_0 + I_0 = 1. \tag{2.2.10}$$

Notice that non-dimensionalizing the SI model, led to a change in how large we can make the total population, in that the number of susceptible and infected individuals is bounded by $N_0$ in Eq.(2.2.8) so that it cannot exceed one.

Next we can use Eq.(2.2.4) and Eq.(2.2.8) to reduce the system of equations Eq.(2.2.6), into a single equation for $I$. From Eqs.(2.2.4), (2.2.8) it follows that $S + I = N = N_0 = 1$ so that $S = 1 - I$ and the ODE for $I$ in Eq.(2.2.6) reduces to

$$\frac{dI}{dt} = (1 - I)I, \quad I(0) = I_0 \geq 0. \tag{2.2.11}$$

This ODE for $I$ has two equilibrium points $I = 0$ and $I = 1$. A straightforward linearized analysis shows that $I = 0$ is an unstable equilibrium and $I = 1$ is a stable equilibrium. Moreover, this ordinary differential equation is the famous logistic equation of Verhulst [25]. Its solution is well-known and can be obtained by separation of variables from which we get the following

$$I(t) = \frac{I_0}{(1 - I_0)\, e^{-t} + I_0} \tag{2.2.12}$$

and therefore

$$S(t) = 1 - I(t) = \frac{(1 - I_0)e^{-t}}{(1 - I_0)e^{-t} + I_0}. \tag{2.2.13}$$

With this formula it is clear to see that as $t$ goes to infinity

$$\lim_{t\to\infty} I(t) = \lim_{t\to\infty} \frac{I_0}{(1 - I_0)e^{-t} + I_0} = \frac{I_0}{I_0} = 1 \tag{2.2.14}$$

and

$$\lim_{t\to\infty} S(t) = \lim_{t\to\infty} \frac{(1 - I_0)e^{-t}}{(1 - I_0)e^{-t} + I_0} = 0. \tag{2.2.15}$$

This means that for the non-dimensionalized SI model, all individuals will become infected as time goes to infinity.

If we revert back to the dimensional variable then the formulas for $I(t)$ and $S(t)$ become

$$I(t) = \frac{I_0 N_0}{a(N_0 - I_0)\, e^{-aN_0 t} + I_0} \tag{2.2.16}$$

$$S(t) = \frac{aN_0(I_0 N_0)e^{-aN_0 t}}{a(N_0 - I_0)\, e^{-aN_0 t} + I_0}. \tag{2.2.17}$$

In this case the limiting behavior of $I(t)$ and $S(t)$ as $t$ goes to infinity becomes

$$\lim_{t\to\infty} I(t) = \lim \frac{I_0 N_0}{(N_0 - I_0)e^{-aN_0 t} + I_0} = \frac{I_0 N_0}{I_0} = N_0 \tag{2.2.18}$$

and

$$\lim_{t\to\infty} S(t) = \lim_{t\to\infty} \frac{aN_0(I_0N_0)e^{-aN_0t}}{a(N_0 - I_0)\, e^{-aN_0t} + I_0} = 0. \tag{2.2.19}$$

Thus the simple SI model predicts that eventually everyone will become infected, no matter how small the initial value of the infected class is. This is shown graphically in Fig 2.1 where we have $N_0 = 1$ individuals for the total population, and an initial susceptible and infected class that is, $S_0 = 0.99$, $I_0 = 0.01$

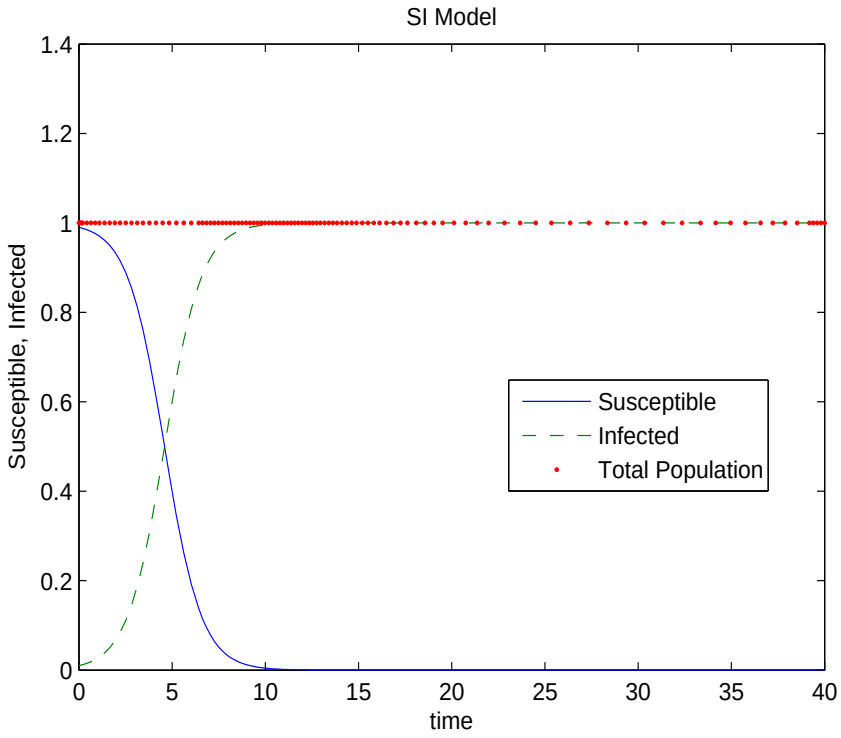


Figure 2.1: Plot of the SI epidemic system. It has a population size of $N_0 = 1$ with $S_0 = 0.99$ and $I_0 = 0.01$. The curves indicate the change in population levels for each class. As time increases, all the individuals in the population will become infected
.

## 2.3 SIR Model

Next we look at the slightly more complicated SIR model. The main difference between the SI model and the SIR model is the treatment of the infected class which no longer stay infected but recover. Once again some assumptions must be made. With $S(t)$, $I(t)$, and $R(t)$ representing the number of individuals in the susceptible ($S$), infected ($I$) and recovered ($R$) classes respectively, and with the total population $N(t)$ given as $N(t) = S(t) + I(t) + R(t)$, we assume that:

1. The rate of growth of the recovered class is given by the reaction mechanism

$$S + I \xrightarrow{a} I \xrightarrow{b} R$$

and the reaction rates in each reaction given by the law of mass action. From the first reaction it follows that the increase of the infected class is at a rate proportional to the number of infected and susceptible, hence $aSI$ where $a > 0$ is a constant parameter, and is known as the infection rate. The susceptible are lost at the same rate. From the second reaction it follows that the rate at which the infected class becomes part of the recovered class is proportional to the number of infected individuals, $bI$ where $b > 0$ is a constant, and is known as the removal rate.

2. No other birth or death mechanism is assumed in the model (e.g. Malthusian or logistic growth for $S$)

Using all the assumptions stated above, we get the SIR model, which is

$$\begin{aligned} \frac{dS}{dt} &= -aSI \\ \frac{dI}{dt} &= aSI - bI \\ \frac{dR}{dt} &= bI \end{aligned} \tag{2.3.1}$$

with initial conditions

$$S(0) = S_0 \geq 0, \quad I(0) = I_0 \geq 0, \quad \text{and} \quad R(0) = R_0 = 0. \tag{2.3.2}$$

This is known as the classic Kermack-McKendrick model [14]. The fixed population is built into the model, and when adding the equations we get,

$$\frac{dN}{dt} = \frac{dS}{dt} + \frac{dI}{dt} + \frac{dR}{dt} = -aSI + aSI - bI + bI = 0 \tag{2.3.3}$$

so that

$$N(t) \equiv N(0) = N_0 = S_0 + I_0 + R_0 \tag{2.3.4}$$

where $N_0$ is the total size of population. It follows that $S$, $I$, $R$, are bounded by $N_0$ from above and $N$ is conserved.

Next we simplify Eq.(2.3.1) through non-dimensionalization of the system. To do so we introduce the following non-dimensional variables

$$\widetilde{I} = \frac{I}{N_0}, \qquad \widetilde{S} = \frac{S}{N_0}, \qquad \widetilde{R} = \frac{R}{N_0}, \qquad \widetilde{t} = a(N_0)t \tag{2.3.5}$$

where $N_0 = S_0 + I_0 + R_0$. If we define $\widetilde{N}(t) = \widetilde{S}(t) + \widetilde{I}(t) + \widetilde{R}(t)$ then it follows from Eq.(2.3.4) that

$$\widetilde{N}(t) = \frac{N(t)}{N_0} \equiv 1. \tag{2.3.6}$$

Next we introduce the non-dimensional variables from Eq.(2.3.5) into Eq.(2.3.1)

$$\begin{aligned} a(N_0)^2 \frac{d\widetilde{S}}{d\widetilde{t}} &= -a(N_0)^2 \widetilde{S}\widetilde{I} \\ a(N_0)^2 \frac{d\widetilde{I}}{d\widetilde{t}} &= -a(N_0)^2 \widetilde{S}\widetilde{I} - bN_0\widetilde{I} \\ a(N_0)^2 \frac{d\widetilde{R}}{d\widetilde{t}} &= -bN_0\widetilde{I}. \end{aligned} \tag{2.3.7}$$

Next we let $c = (b/aN_0)$, drop the tildes for notational simplicity, and then we arrive at the non-dimensionalized SIR model which is

$$\begin{aligned} \frac{dS}{dt} &= -SI \\ \frac{dI}{dt} &= SI - cI \\ \frac{dR}{dt} &= cI \end{aligned} \tag{2.3.8}$$

with initial conditions

$$S(0) = S_0 \geq 0, \quad I(0) = I_0 \geq 0, \quad \text{and} \quad R(0) = R_0 = 0 \tag{2.3.9}$$

and the total non-dimensional population being one

$$N(t) \equiv N_0 = S_0 + I_0 + R_0 = 1. \tag{2.3.10}$$

It is interesting to note that if $c = 0$ we get back the SI model. Since $c = (b/aN_0)$ then $c$ is small when $b$ is small compared to $aN_0$. Under these conditions we could expect the SIR model to be well approximated by the SI model, at least for $S \gg c$.

The SIR system in Eq.(2.3.8) is weakly coupled in the sense that the differential equations for $S$, $I$ do not involve $R$; knowledge of $S$ and $I$ suffice to determine $R$. For this reason a complete understanding of the SIR model can be gained by studying the reduced SIR system

$$\begin{aligned} \frac{dS}{dt} &= -SI \\ \frac{dI}{dt} &= (S - c)I \end{aligned} \tag{2.3.11}$$

with initial conditions

$$S(0) = S_0 \geq 0 \quad \text{and} \quad I(0) = I_0 \geq 0. \tag{2.3.12}$$

The reduced SIR system has a continuum of non-isolated equilibrium solutions given by

$$S(t) \equiv S_0 \quad \text{and} \quad I(t) \equiv 0 \tag{2.3.13}$$

This set of equilibrium solutions describe the positive S-axis in the SI-plane. It is also clear that a special solution of the reduced SIR system is given by

$$S(t) \equiv 0 \quad \text{and} \quad I(t) = I_0 e^{-ct} \tag{2.3.14}$$

which describes a segment of the positive I-axis in the SI-plane. Since the positive S-axis and the positive I-axis are composed of solutions of the reduced SIR system, it follows that the first quadrant is an invariant region in the SI plane, that is, if $S(0) = S_0 \geq 0$ and $I(0) = I_0 \geq 0$ than $S(t) \geq 0$ and $I(t) \geq 0$ for all $t \geq 0$.

In addition, if $(F, G) = (-SI, (S-c)I)$ denotes the right hand side of Eq.(2.3.8), then on the line $S = c$ the vector field $(F, G)$ assumes the value

$$(F, G) = (-cI, 0) \tag{2.3.15}$$

which points into the strip $0 \leq S \leq c$, $0 \leq I < \infty$. This is enough to guarantee that the strip $0 \leq S \leq c$, $0 \leq I < \infty$ is also an invariant region: if $S(0) = S_0 \leq c$ and $I(0) = I_0 \geq 0$ then $0 \leq S(t) \leq c$ and $0 \leq I(t) < \infty$ for $0 \leq t < \infty$.

Using this information we can describe qualitatively what is an epidemic in the context of the SIR model. We can say that there is an **epidemic outbreak** if there is a $T_* > 0$ so that $I(t) > I_0$ for $0 \leq t \leq T_*$. Clearly if $0 \leq I_0 < \infty$ and $0 \leq S_0 \leq c$, then $0 \leq I(t) < \infty$ and $0 \leq S(t) \leq c$ for all $0 \leq t < \infty$, but on virtue of the fact that

$$\frac{dI}{dt} = (S - c)I \leq 0 \tag{2.3.16}$$

it follows that $0 \leq I(t) \leq I_0$ for all $0 \leq t < \infty$. In other words, if $S_0 \leq c$ then there is no epidemic outbreak in the SIR model. On the other hand if $0 < I_0 < \infty$ and $c < S_0 < \infty$ then we have

$$\left.\frac{dI}{dt}\right|_{t=0} = (S-c)I\Big|_{t=0} = (S_0 - c)I_0 > 0 \tag{2.3.17}$$

and at least for a small time interval $0 \leq t \leq T_*$ we have

$$I(t) > I(0) = I_0. \tag{2.3.18}$$

In other words, if $c < S_0 < \infty$ then there is an epidemic outbreak in the SIR model.

By eliminating $t$ in the reduced SIR system in Eq.(2.3.16) it follows that the orbits are described by the curves

$$\frac{dI}{dS} = \frac{c-S}{S} \tag{2.3.19}$$

with solution

$$I = c\ln s - s + d \tag{2.3.20}$$

with $d$ as an arbitrary constant. It follow from Eq.(2.3.19) that

$$\begin{aligned} \frac{dI}{dS} &= 0 \quad \text{iff} \quad S = c \\ \frac{dI}{dS} &> 0 \quad \text{iff} \quad 0 < S < c \\ \frac{dI}{dS} &< 0 \quad \text{iff} \quad c < S < \infty. \end{aligned} \tag{2.3.21}$$

Therefore the orbit described by Eq.(2.3.20) crosses the S-axis at two equilibrium points $(S_1, 0)$, $(S_2, 0)$ with $0 < S_1 < c < S_2$, $I(S)$ is increasing on $S_1 \leq S \leq c$, has a maximum at $S = c$, and it is decreasing on $c \leq S \leq S_2$, compare with Fig

2.2. Moreover, since $S'(t) = -SI < 0$ then $S(t)$ decreases in time and the orbits described by Eq.(2.3.20) are traversed from right to left, starting at $(S_2, 0)$ and ending at $(S_1, 0)$. From here it follows that all the equilibrium points $(S_1, 0)$ with $0 \leq S_1 < c$ are stable and all of the equilibrium points $(S_2, 0)$ with $c < S_2 < \infty$ are unstable. This is clearly illustrated in the phase plane portrait of the reduced SIR system depicted in Fig 2.2.

Finally, Fig 2.3 depicts two representative solutions of the SIR model for the value $c = 0.5$. The top figure displays a typical solution with $S(0) = S_0 > c$, in which case there is an epidemic outbreak as clearly displayed by the initial increase of the infected population $I(t)$. On the other hand, the bottom figure displays a typical solution with $S(0) = S_0 < c$. In this case the infected population $I(t)$ decreases monotonically to zero and there is no epidemic outbreak of the SIR system.

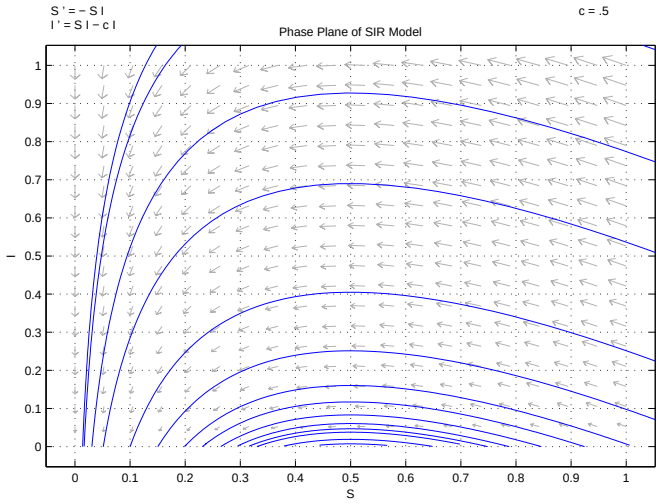


Figure 2.2: Phase plane diagram for the reduced SIR system showing several solution trajectories for $c = 0.5$. Notice all the orbits take a maximum value of $I$ at $S = c = 0.5$. Also notice that the equilibrium points $(S_*, 0)$ on the S-axis are stable if $S_* < c = 0.5$ and unstable if $S_* > c = 0.5$

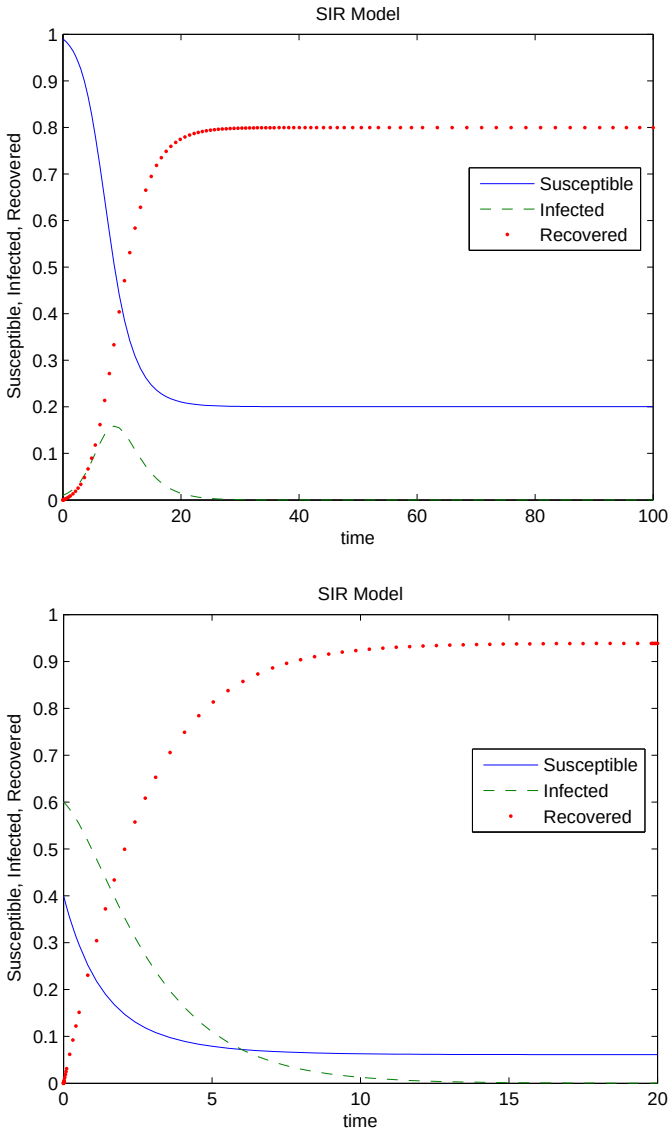


Figure 2.3: Plots of the solution of the SIR system exemplifying the role of the critical parameter $c$ ($c = 0.5$) in the outbreak of an epidemic. Top figure: $S_0 = 0.99$, $I_0 = 0.01$, and $R_0 = 0$ so that ($S_0 > c$). There is an epidemic outbreak with the maximum of infected individuals at about $t = 10$. Bottom figure: $S_0 = 0.4$, $I_0 = 0.6$, and $R_0 = 0$ so that ($S_0 < c$). The number of infected individuals decreases monotonically to zero and there is no epidemic outbreak.

# Chapter 3

# Diffusive SI Model

## 3.1 Introduction

It is a fact that the spread of infectious diseases is effected by the spatial displacement of populations so that a practical model of the spread of infectious diseases should incorporate the effects. These spatial displacements can occur either naturally, being that species have a proneness for movement or due to the disease itself, with individuals wanting to move away from infected areas and hopefully avoid the infection. Now we must consider how we want to model the spread of the population. The use of diffusion is the simplest mechanism used to model the spread of the population. It follows that the system of ordinary differential equations coupled with this diffusion leads naturally to a system of partial differential equations and to the so-called reaction diffusion equations for the study of the spatial spread of infectious diseases. Examples of the case of reaction-diffusion equations to model spatial spreading of infectious diseases can be seen in many epidemiological and ecological contexts. For example, the study of the spread of rabies within a population of foxes as given by Anderson et al [1], Källén et al [12], Murray et al [19], in which the following diffusive

SI model, which was introduced by Källén [12], is used

$$\begin{aligned} s_t &= -is \\ i_t &= i_{xx} + is - \lambda i \end{aligned} \tag{3.1.1}$$

where $s$ denotes the density of the susceptible foxes and $i$ the density of the infected foxes. With this model the infected foxes disperse while the susceptible foxes do not disperse. We also include in this model for the infected individuals built in mortality rate, that is, a decrease to the infected fox population. Murray [21] expanded on the model given by Eq.(3.1.1) by introducing simple logistic growth which represents the foxes reproduction in which we get the following model

$$\begin{aligned} s_t &= -is + bs(1-s) \\ i_t &= i_{xx} + is - \lambda i. \end{aligned} \tag{3.1.2}$$

The diffusive SI model can also be applied to the European Plague or Black Death of the 14th century and was done so by Murray [20],[21]. With the Black Death it was common place for individuals to move or disperse from an area where the infectious disease was flourishing to a location not previously exposed to the disease, with the goal being to avoid the infection and this would ultimately lead to limiting the effect of the epidemic so that it would be contained or confined to that particular area. However, with the European plague there was an incubation period meaning that symptoms did not show up for some amount of time and unfortunately this meant that infected as well as susceptible individuals relocated which obviously attributed to the infectious disease being introduced into new areas or populations not previously subjected to the disease and therefore helped in creating massive epidemic with millions of individuals dying. Now, modeling this includes adding the susceptible diffusion previously mentioned and having equal diffusivities for the

susceptible and infected individuals in Eq.(3.1.1), and from this we have the following diffusive SI model given by Murray [21]

$$\begin{aligned} s_t &= s_{xx} - is \\ i_t &= i_{xx} + is - \lambda i. \end{aligned} \tag{3.1.3}$$

Here, we want to focus attention on the diffusive SI model

$$\begin{aligned} s_t &= D_s\, s_{xx} - asi \\ i_t &= D_i\, i_{xx} + asi, \end{aligned} \tag{3.1.4}$$

which is a special case of the general reaction diffusion system

$$\begin{aligned} s_t &= D_s\, s_{xx} + f(s,i) \\ i_t &= D_i\, i_{xx} + g(s,i). \end{aligned} \tag{3.1.5}$$

For example, Eq.(3.1.1) with $\lambda = 0$ compares to Eq.(3.1.4) with $a = 1$, $D_s = 0$ and $D_i = 1$, Eq.(3.1.2) with $\lambda = 0$ and $b = 0$ also compares to Eq.(3.1.4) with $a = 1$, $D_s = 0$ and $D_i = 1$ and finally Eq.(3.1.3) with $\lambda = 0$ relates to Eq.(3.1.4) with $a = 1$, $D_s = 1$ and $D_i = 1$.

With this diffusive model we have combined the ordinary differential equations that made up the SI system seen in Chapter 2 with the simple diffusion and this gave us the system of partial differential equations in Eq.(3.1.4). Now, a problem that is associated with these type of diffusive SI models is the existence of traveling waves in an infinite domain, i.e. solutions to the diffusive models of the form

$$\begin{aligned} s(x,t) &= s(x - ct) \\ i(x,t) &= i(x - ct) \end{aligned} \tag{3.1.6}$$

where $c$ is the speed of propagation of the wave. Extensive studies have been done on traveling waves including the propagation of the plague with context to the SI model with diffusion, Noble [23], and the spread of rabies among foxes, MacDonald [18].

If we have $D_s = D_i = D$ and also $s + i \equiv N_0$ in Eq.(3.1.4) then the associated traveling waves are given as the simpler Fisher equation

$$i_t = D\, i_{xx} + a(N_0 - i)i \tag{3.1.7}$$

which has been studied in great detail in the pioneer works of Fisher [6] and Kolmogoroff et al. [17]. These studies revealed the existence of traveling waves for any speed $c$ that is bigger than some minimal speed $c_*$ such that

$$c \geq c_* = 2\sqrt{DaN_0}. \tag{3.1.8}$$

In more recent work Murray [21] investigated the spread of the European plague within the context of a traveling wave for the reaction-diffusion system in Eq.(3.1.3). In this work, Murray showed that traveling waves exist for any speed $c$ larger then the minimal speed $c_*$ given by

$$c \geq c_* = 2\sqrt{1 - \lambda} \quad \text{with} \quad \lambda < 1. \tag{3.1.9}$$

It was also shown by Murray [21] that for $\lambda > 1$ that there is no traveling wave and so for there to be propagation of an epidemic, $\lambda < 1$, yielding a threshold criterion. In the same work, Murray was able to estimate the speed propagation, $V$, of the Black Plague to be approximately

$$V \approx 140 \text{ miles/year}. \tag{3.1.10}$$

Traveling waves for reaction diffusion equations have been extensively studied and excellent expositions can found in Fife [6], Hoppensteadt [10], [11], and Murray [19], [20].

In the present chapter we will concentrate instead on the diffusive SI model on a bounded domain, rather than a infinite domain

$$\begin{aligned} s_t &= D_s\, s_{xx} - asi \\ i_t &= D_i\, i_{xx} + asi \end{aligned} \tag{3.1.11}$$

with $0 \leq x \leq L$ and $0 < t < \infty$. Here $s = s(x,t)$ and $i = i(x,t)$ represent the density of the susceptible and infected class per unit length respectively, also $D_s$ and $D_i$ are the the diffusion coefficients for the susceptible and infected class in that order so that each class can diffuse with either equal or non-equal diffusivities, and $a$ denotes the virulence strength of the disease.

This system is supplemented with Neumann (no flux) boundary conditions at both end points $x = 0, L$

$$\begin{aligned} &s_x(0,t) = 0 \qquad \text{and} \qquad s_x(L,t) = 0 \\ &i_x(0,t) = 0 \qquad \text{and} \qquad i_x(L,t) = 0 \end{aligned} \tag{3.1.12}$$

and with initial conditions

$$s(x,0) = s_0(x) \geq 0 \qquad \text{and} \qquad i(x,0) = i_0(x) \geq 0. \tag{3.1.13}$$

Associated with the densities $s(x,t)$ and $i(x,t)$ are the total number of susceptible $S(t)$, the total number of infected $I(t)$ and the total number of individuals that make up the population $N(t)$, defined by

$$\begin{aligned} S(t) &= \int_0^L s(x,t)\, dx \\ I(t) &= \int_0^L i(x,t)\, dx \\ N(t) &= S(t) + I(t). \end{aligned} \tag{3.1.14}$$

From Eq.(3.1.11) we can prove that $N(t)$ is a conserved quantity, i.e. $N(t) \equiv N(0) = N_0 = S_0 + I_0$. In fact, if we differentiate $N(t)$ in Eq.(3.1.13) with respect to $t$, we get

$$\begin{aligned}
\frac{dN}{dt} &= \frac{dS}{dt} + \frac{dI}{dt} \\
&= \int_0^L s_t \, dx + \int_0^L i_t \, dx \\
&= \int_0^L (D_s \, s_{xx} - asi) \, dx + \int_0^L (D_i \, i_{xx} + asi) \, dx \\
&= D_s \, s_x \Big|_0^L + D_i \, i_x \Big|_0^L - \int_0^L asi \, dx + \int_0^L asi \, dx \\
&= 0,
\end{aligned}$$

where we utilized the Neumann boundary conditions, Eq.(3.1.11), to evaluate the boundary contributions at the end points $x = 0, L$. Since $N(t)$ does not change in time we conclude that $N(t)$ is conserved for all times,

$$N(t) \equiv N(0) = N_0 = S_0 + I_0, \tag{3.1.15}$$

where $N_0$ is the total initial population. In particular, it follows that $S$ and $I$ are bounded above by $N_0$.

It is interesting to observe that if the initial data is homogenous in space, $s(x, 0) = s_0$, $i(x, 0) = i_0$, then the diffusive SI model admits a spatially homogeneous solution $s(x, t) = s(t)$ and $i(x, t) = i(t)$. Moreover, in this case the integrated values of $s(t)$ and $i(t)$ in Eq.(3.1.5) become

$$S(t) = Ls(t) \tag{3.1.16}$$

$$I(t) = Li(t) \tag{3.1.17}$$

and they satisfy the SI ODE system studied in Chapter 2, namely

$$\begin{aligned} \frac{dS}{dt} &= -\alpha SI, \qquad S(0) = Ls_0 \\ \frac{dI}{dt} &= \alpha SI, \qquad I(0) = Li_0 \end{aligned} \tag{3.1.18}$$

with $\alpha = a/L$.

Next we simplify Eq.(3.2.1) by non-dimensionalization of the system. To do so we introduce the non-dimensional variables

$$\widetilde{s} = \frac{sL}{N_0}, \quad \widetilde{i} = \frac{iL}{N_0}, \quad \widetilde{t} = \frac{aN_0\, t}{L}, \quad \widetilde{x} = \frac{x}{L} \tag{3.1.19}$$

where $N_0 = S_0 + I_0$. If we define

$$\widetilde{S}(t) = \frac{S(t)}{N_0}, \quad \widetilde{I}(t) = \frac{I(t)}{N_0}, \quad \widetilde{N}(t) = \frac{N(t)}{N_0} \tag{3.1.20}$$

where $S(t)$, $I(t)$, and $N(t)$ are given in Eq.(3.2.5), then it follows from Eq.(3.2.6) that

$$\widetilde{N}(t) = \frac{N(t)}{N_0} \equiv 1. \tag{3.1.21}$$

Next we introduce the non-dimensional variables for Eq.(3.2.7) into Eq.(3.2.1)

$$\begin{aligned} a\left(\frac{N_0}{L}\right)^2 \frac{\partial \tilde{s}}{\partial \tilde{t}} &= D_s\, \frac{N_0}{L^3}\, \frac{\partial^2 \tilde{s}}{\partial \tilde{x}^2} - a\left(\frac{N_0}{L}\right)^2 \tilde{s}\tilde{i} \\ a\left(\frac{N_0}{L}\right)^2 \frac{\partial \tilde{i}}{\partial \tilde{t}} &= D_i\, \frac{N_0}{L^3}\, \frac{\partial^2 \tilde{i}}{\partial \tilde{x}^2} + a\left(\frac{N_0}{L}\right)^2 \tilde{s}\tilde{i}. \end{aligned} \tag{3.1.22}$$

Now we drop the tildes for notational simplicity, and then we arrive at the **non-dimensionalized SI model**

$$\begin{aligned} s_t &= d_s\, s_{xx} - si \\ i_t &= d_i\, i_{xx} + si \end{aligned} \tag{3.1.23}$$

where $d_s = (D_s/aN_0L)$ and $d_i = (D_i/aN_0L)$ are the non-dimensional diffusivities and with initial data given by with initial conditions

$$s(x,0) = s_0(x) \geq 0 \quad \text{and} \quad i(x,0) = i_0(x) \geq 0 \tag{3.1.24}$$

with $0 \leq x \leq 1$ and with Neumann boundary conditions

$$\begin{aligned} s_x(x,t)|_{x=0,1} &= 0 \\ i_x(x,t)|_{x=0,1} &= 0. \end{aligned} \tag{3.1.25}$$

Again we remark that in accordance with Eq.(3.1.15), $N(t)$ is constant, and the total population has been normalized to the value one

$$N(t) = N_0 = S_0 + I_0 = \int_0^1 s(x,0)\, dx + \int_0^1 i(x,0)\, dx \equiv 1. \tag{3.1.26}$$

In the next section we are going to study the diffusive SI system, Eqs.(3.2.10-12) for the cases of equal ($d_s = d_i$) and different ($d_s \neq d_i$) diffusivities. For this study it seems natural to chose spatially homogeneous initial data $s_0$ for the susceptible $s(x,t)$,

$$s(x,0) = s_0, \qquad 0 \leq x \leq 1 \tag{3.1.27}$$

and a normalized gaussian centered at $x = 1/2$ for the infected $i(x,t)$ (to represent a focus of infection)

$$i(x,0) = i_0 \, \frac{e^{-\sigma(x-1/2)^2}}{\displaystyle\int_0^1 e^{-\sigma(x-1/2)^2}\, dx} = i_0 \, g(x) \quad \text{with} \quad \sigma = 10,000. \tag{3.1.28}$$

In all the calculations below we will use the values $i_0 = 0.01$ (1% infected population) and $s_0 = 0.99$ (99% susceptible population) for the initial values. Notice that for this large value of $\sigma$ the Gaussian is highly concentrated about $x = 1/2$, with the area $A$ over the interval $0 \leq x \leq 1$,

$$A = \int_0^1 e^{-\sigma(x-1/2)^2}\, dx = \int_0^1 e^{-10,000(x-1/2)^2}\, dx \cong 0.0174565 \tag{3.1.29}$$

accounting for almost all of the total area of the Gaussian

$$\int_{-\infty}^{\infty} e^{-\sigma(x-1/2)^2}\, dx = \sqrt{\frac{\pi}{\sigma}} = \sqrt{\frac{\pi}{10,000}} \cong 0.0177245 \tag{3.1.30}$$

so that the difference is negligible

$$\int_{-\infty}^{\infty} e^{-10{,}000(x-1/2)^2}\, dx - \int_{0}^{1} e^{-10{,}000(x-1/2)^2}\, dx = 0.00027.$$

A plot of the normalized Gaussian

$$g(x) = \frac{e^{-\sigma(x-1/2)^2}}{\displaystyle\int_0^1 e^{-\sigma(x-1/2)^2}\, dx} \tag{3.1.31}$$

for $\sigma = 10,000$ is given in Fig.(3.1). Notice that the Gaussian is highly peaked, in effect an approximation of the Dirac delta function, so that the infected population is almost exclusively concentrated at $x = 1/2$ initially.

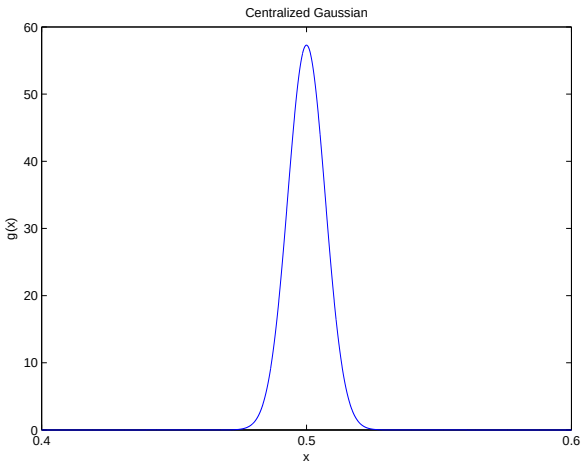


Figure 3.1: Plot of the Normalized Gaussian centered at $x = 1/2$ given by Eq.(3.1.31), taken between the interval [0.4,0.6] to show its high concentration. The function $g(x)$ is concentrated almost entirely around the center point. The total area of $g(x)$ over the interval $0 \leq x \leq 1$ is $\int_0^1 g(x)\, dx = 1$

## 3.2 Numerical Solution Procedure

In the next two sections we will study the diffusive SI system, Eq.(3.1.10-12) with special initial data given by Eqns.(3.1.27, 3.1.28), and particular attention will be given to consider the situations with equal and different diffusivities. The diffusive SI system is solved numerically with the PDE package *pdepe*, which solves parabolic/elliptic partial differential equations in MATLAB. The package implements an adaptive finite element method and is well suited for the solution of reaction-diffusion equations. Next we describe briefly how we used the PDE package *pdepe* to solve numerically the diffusive SI system (and the diffusive SIR system in the next chapter).

The MATLAB package *pdepe* solves parabolic and elliptic partial differential equations in one space dimension $x$ and time $t$, of the form

$$c(x,t,u_x)\frac{\partial u}{\partial t} = x^{-m}\frac{\partial}{\partial x}\left(x^m f(x,t,u,u_x)\right) + g(x,t,u,u_x) \tag{3.2.1}$$

where $u(x,t)$ is a vector function with $n$ components (with $n = 2$ for the SI model whereas $n = 3$ for the SIR model). The vector function $f(x,t,u,u_x)$ represents a generalization of Fourier's law for the heat flux and can incorporate heat fluxes $K(u)u_x$, and spatio-temporal inhomogeneities through variations in $(x,t)$. The vector function $g(x,t,u,u_x)$ can incorporate reaction, advection, and inhomogeneities where $a \leq x \leq b$ and $t_0 < t < t_f$. The integer $m$ can be equal to $0, 1, 2$, which translates to slab, cylindrical or spherical symmetry, respectively. For the interval $a \leq x \leq b$ and initial time $t = t_0$, the solution must satisfy $u(x,t_0) = u_0(x)$. At the boundary $x = a$ or $x = b$, for $t_0 < t < t_f$, the solution components satisfy a boundary condition of the form

$$p(x,t,u) + q(x,t)f(x,t,u_x) = 0. \tag{3.2.2}$$

These are rather general boundary conditions that include both Dirichlet boundary conditions ($p(x,t,u) = u,\ q(x,t) = 0$) and Neumann boundary conditions

($p(x,t,u) = 0,\ q(x,t) = 1,\ f(x,t,u) = D\ u_x$). For the diffusive SI system given to us in Eq.(3.1.13), we have two equations so we need to write the diffusive SI system in the following form and in a way that *pdepe* can understand

$$\begin{pmatrix} 1 & 0 \\ 0 & 1 \end{pmatrix} \times \frac{\partial}{\partial t} \begin{pmatrix} s \\ i \end{pmatrix} = \frac{\partial}{\partial x} \begin{pmatrix} \frac{\partial s}{\partial x} \\ \frac{\partial i}{\partial x} \end{pmatrix} + \begin{pmatrix} -si \\ si \end{pmatrix}, \tag{3.2.3}$$

and so for Eq.(3.2.1) we assign the following values for $m$, $c$, $f$, and $g$ in the diffusive SI system

$$\begin{aligned} m &= 0 \\ c(x,t,u,u_x) &= \begin{pmatrix} 1 \\ 1 \end{pmatrix} \\ f(x,t,u,u_x) &= \begin{pmatrix} s_x \\ i_x \end{pmatrix} \\ g(x,t,u,u_x) &= \begin{pmatrix} -si \\ si \end{pmatrix}. \end{aligned} \tag{3.2.4}$$

The boundary conditions for the diffusive SI system which are the Neumann boundary conditions given by Eq.(3.1.12) with $L = 1$ are set up in *pdepe* in the following fashion

$$\begin{aligned} p(0,t,u) &= \begin{pmatrix} 0 \\ 0 \end{pmatrix} \\ q(0,t) &= \begin{pmatrix} 1 \\ 1 \end{pmatrix} \\ p(1,t,u) &= \begin{pmatrix} 0 \\ 0 \end{pmatrix} \\ q(1,t) &= \begin{pmatrix} 1 \\ 1 \end{pmatrix}. \end{aligned}$$

Now, part of *pdepe*'s argument list is the vector *xmesh* which is a set of points in the interval $a \leq x \leq b$ such that $xmesh(1) = a$ and $xmesh(end) = b$ and where $xmesh(i) < xmesh(i+1)$. This specifies the values for $x$ at which the numerical solution is computed. For our system, we have $a = 0$ and $b = 1$ and with the interval $0 \leq x \leq 1$ consisting of one hundred points in space. The vector *tspan* defines the points in time within the interval $t_0 < t < t_f$ where the solution is to be presented, with $tspan(1) = t_0$, $tspan(end) = t_f$, and $tspan(i) < tspan(i+1)$. For us, $t_0 = 0$ and $t_f$ may vary but with one hundred time steps for all values between $0 < t < t_f$. We create individual functions in MATLAB for the initial conditions, boundary conditions, and the equations that make up the diffusive SI system. We then create an all encompassing function that calls all of these separate functions and uses *pdepe*, at which point we are provided with solutions to the equations which we will call *sol*. Now, the output argument *sol* is a 3-D array such that $sol(j,k,i)$ is the approximation to the ith component of $u$ at the point $t = tspan(j)$ and $x = xmesh(k)$. Putting all this together we obtain numerical solutions to describe the behavior of the infected and susceptible individuals over the space $x$ and time $t$.

In order to assess the role of diffusion in the propagation of the epidemic we need to compare the solution of the diffusive SI model versus the solution of the SI system. For this purpose we need to compute the total populations of susceptible and infected individuals, $S(t)$, $I(t)$, given by Eq.(3.1.14) with $L = 1$.

$$\begin{aligned} S(t) &= \int_0^1 s(x,t)\,dx \\ I(t) &= \int_0^1 i(x,t)\,dx \end{aligned} \tag{3.2.5}$$

and compare them with the corresponding values $S(t)$, $I(t)$ obtained for the SI system in Chapter 2. The calculation of the integrals in Eq.(3.2.5) is done in MATLAB using the built in function *trapz*, which yields a numerical approximation of the integrals

through the use of the trapezoidal rule. By applying *trapz* at the predetermined times given by *tspan* we obtain the time evolution of the population totals $S(t)$ and $I(t)$ of the diffusive SI model that are needed for comparison with the SI system.

## 3.3 Diffusive SI Model with Arbitrary Diffusivities

In this section we concern ourselves with the actions of the susceptible and infected individuals that exist within the diffusive SI system with arbitrary diffusivities and ultimately, we want to compare and contrast this PDE system with the ODE SI system of Chapter 2 by assessing the effects arising from the introduction of diffusion. The diffusivities are given as $d_s$ for the susceptibles and $d_i$ for the infectives. For all numerical experiments we have $s_0 = 0.99$ (99% susceptible population) and $i_0 = 0.01$ (1% infected population). We consider the diffusion coefficients with values $d_i, d_s = 0, 10^{-3}, 10^{-2}, 10^{-1}, 10^{0}, 10^{1}$ spanning five orders of magnitude in parameter space, and including the ranges of strong and weak diffusivities for both the susceptible and infected populations. Here we identified three regions in parameter space, regimes for short, so that all the solutions in the given regime display similar behavior which we will discuss shortly.

To study the effect that diffusion has on the evolution and spread of the infectious disease we will compare the total populations $S(t)$ and $I(t)$ of susceptible and infected individuals in the diffusive SI model with the corresponding values predicted by the SI equations. At this point an observation on the mathematical meaning of this comparison is in order. If we integrate in space the diffusive SI system, Eq.(3.3.1) and

apply the Neumann boundary conditions, we obtain the integro-differential equations

$$\begin{aligned} \frac{dS}{dt} &= -\overline{si} \qquad S(0) = s_0 \\ \frac{dI}{dt} &= \overline{si} \qquad I(0) = i_0 \end{aligned} \tag{3.3.1}$$

where $\overline{si} = \int_0^1 s(x,t)\ i(x,t)\ dx$, with $s(x,t)$, $i(x,t)$ the solution of the diffusive SI model. On the other hand, the SI-model is given by the ODE system

$$\begin{aligned} \frac{dS}{dt} &= -SI \qquad S(0) = S_0 \\ \frac{dI}{dt} &= SI \qquad I(0) = I_0. \end{aligned} \tag{3.3.2}$$

It is clear that the two systems would be equivalent if and only if $\overline{si} = SI$, that is,

$$\int_0^1 s(x,t)\ i(x,t)\ dx = \left(\int_0^1 s(x,t)\ dx\right)\left(\int_0^1 i(x,t)\ dx\right). \tag{3.3.3}$$

However, in general the integral of a product of functions is never equal to the product of the integrals, i.e. Eq.(3.3.4) is never satisfied. Mathematically speaking, the comparison of the diffusive SI model versus the SI model boils down to studying the effects of replacing the integral of a product by the product of the integrals.

The combination of diffusivity parameter values previously mentioned are collected in Table 3.1. The values on the main diagonal correspond to the cases of equal diffusivities, $d_s = d_i$. The farther we move from the main diagonal in the table, the more disparate $d_s$ and $d_i$ are, with the top right corner corresponding to strong diffusion of the susceptibles and weak diffusion of infectives ($d_i \ll d_s$) and the bottom left corner corresponding to weak diffusion of susceptibles and strong diffusion of infectives ($d_i \gg d_s$).

In Table 3.1 we identified three regions (regimes) in parameter space characterized by the distinctive behavior of their solutions. Regime I is characterized by strong I-diffusion. Regime II corresponds to weak SI-diffusion. Finally, Regime III corresponds to weak I-diffusion and strong S-diffusion. The distinctive features of the solutions in these regimes will be considered below. We also remark that the asymmetry displayed in the table is not too surprising if we recall that the initially infective population is highly concentrated, where the susceptible population is uniformly distributed in space, therefore it is natural to expect the infectious propagation dynamics to be more sensitive to changes in the infective diffusivity $d_i$.

It is important to note that the solutions in these regions display common characteristics in their time evolutions. The boundaries of these regions are somewhat blurry in that a case near the boundary could be classified as belonging to another region and could be open to interpretation. Next we proceed to discuss the main features of the three diffusion regimes identified earlier.

Table 3.1: Diffusivity values for the susceptible and infected individuals that are categorized into one of three general numerical solutions depending on the various pairings of these values.

| $d_i \backslash d_s$ | 0 | 0.001 | 0.01 | 0.1 | 1 | 10 |
|---|---|---|---|---|---|---|
| 0 | *II* | *II* | *II* | *III* | *III* | *III* |
| 0.001 | *II* | *II* | *II* | *III* | *III* | *III* |
| 0.01 | *I* | *I* | *I* | *I* | *I* | *I* |
| 0.1 | *I* | *I* | *I* | *I* | *I* | *I* |
| 1 | *I* | *I* | *I* | *I* | *I* | *I* |
| 10 | *I* | *I* | *I* | *I* | *I* | *I* |

## **Regime I** (strong I-diffusion regime)

This regime corresponds to values of $d_s \geq 0$ and $d_i \geq 10^{-2}$ in the numerical experiments and it is characterized by the rapid homogenization of spatial variations in the populations. In particular, the highly concentrated initial population of infectives spreads out quickly and uniformly over the entire spatial domain. This is clearly demonstrated in Fig 3.2, which is a representative case that displays the susceptible and infected population for the case where the diffusivities are $d_s = 10^{-1}$ and $d_i = 1$. After a very short time interval, both $s(x,t)$ and $i(x,t)$ become spatially homogeneous, with $s(x,t)$ decaying to its minimum value $s = 0$, and $i(x,t)$ growing to its maximum value $i = 1$, at about $t = 10$. Once the populations have become spatially homogeneous their evolution in time should follow the SI model. This is clearly demonstrated in Fig 3.3 where the total populations $S(t)$ and $I(t)$ of the diffusive SI model are compared with their counterparts for the SI-model. The results show remarkably good agreement between the values of $S(t)$ and $I(t)$ predicted by both models, with a slight time delay present in the diffusive SI model. In general, this good agreement between the diffusive SI model and the SI-model is consistent, meaning the totals for the populations are insensitive to increases in $d_s$ and $d_i$ for this regime. The results of the numerical experiments also indicate that the SI-model should be strictly valid in the limit when $d \to \infty$ or in mathematical jargon, when $d = \infty$ we can replace the integral of a product by the product of the integrals. Therefore we can replace the diffusive SI model with the simpler SI-model when the diffusivities belong to this regime.

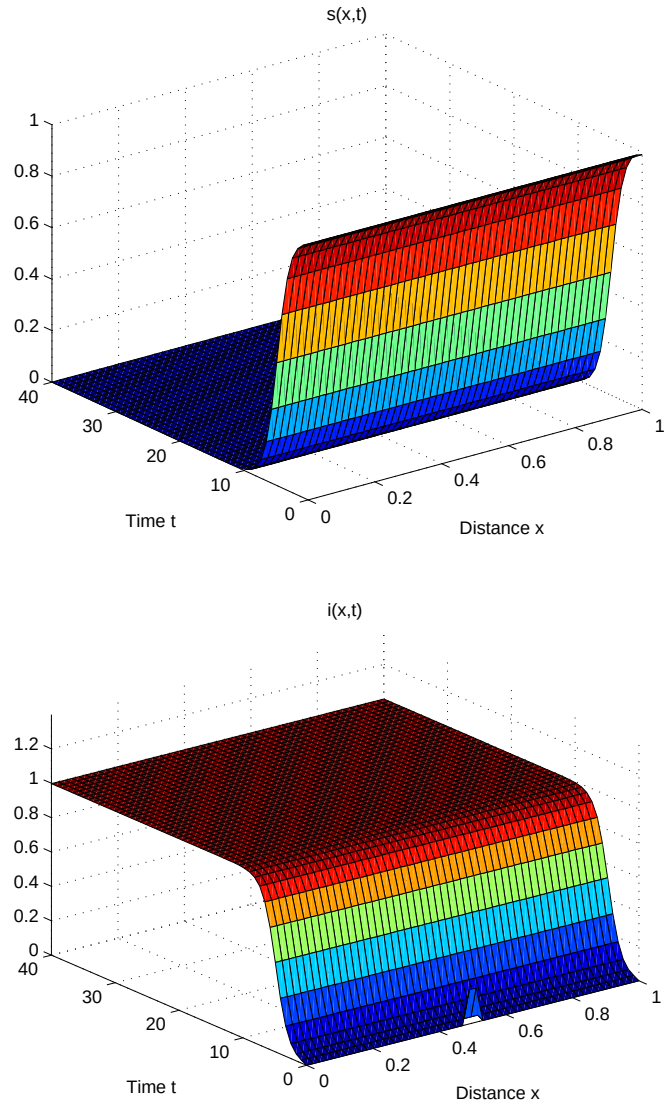


Figure 3.2: Solution of the Diffusive SI model with $d_s = 0.1$ and $d_i = 1$ (regime I: strong I-diffusion). Both populations $s(x,t)$, $i(x,t)$ become spatially homogeneous after a very short adjustment time.

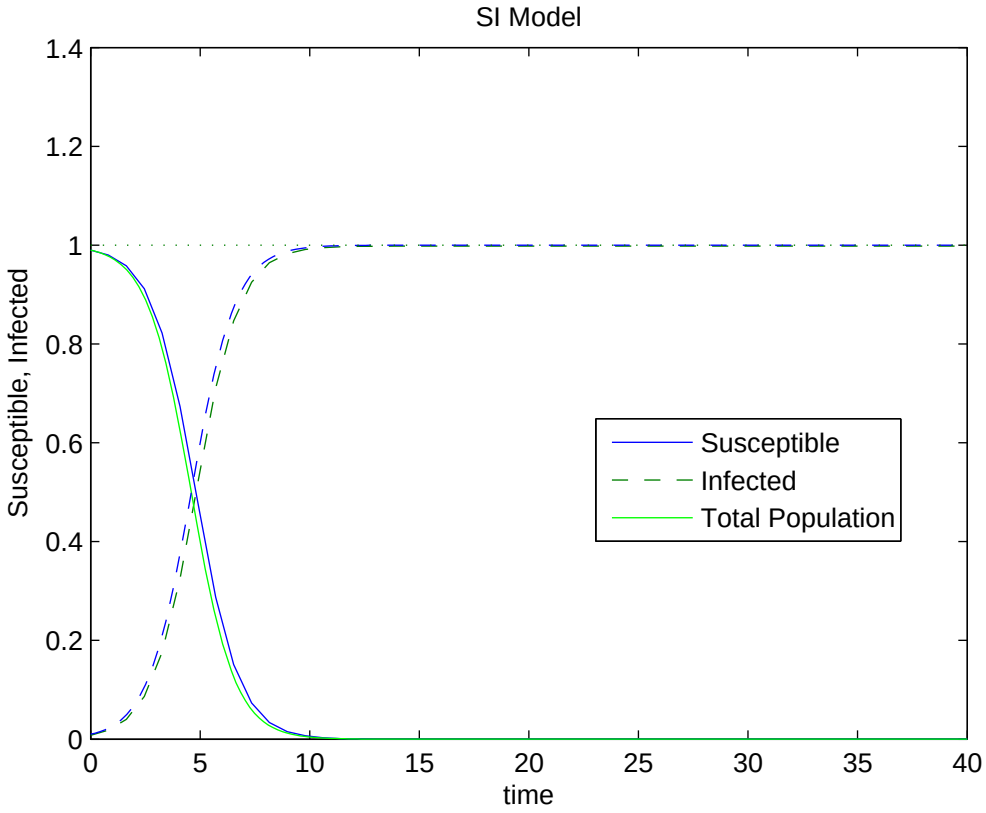


Figure 3.3: Comparison of the totals for the susceptible (S) and infected (I) individuals from the diffusive SI system with $d_s = 0.1$ and $d_i = 1$ (strong I-diffusion regime). Both solutions are in close agreement, with $S(t)$, $I(t)$ from the diffusive model slightly lagging in time.

## **Regime II** (weak SI-diffusion regime)

This regime corresponds to values of $d_s \leq 10^{-2}$ and $d_i \leq 10^{-3}$ in the numerical experiments and is characterized by the slow homogenization of the populations. Fig 3.4 shows the time evolution of the susceptible and infected individuals for $d_s = 10^{-3}$ and $d_i = 10^{-3}$. The small value of the diffusion coefficient results in the slow spread of the highly concentrated population of infected individuals, and this also results in the emergence of inhomogeneities in the population of susceptibles. Although both $s(x,t)$ and $i(x,t)$ are spatially inhomogeneous, these inhomogeneities subside with time and the final fate of the populations is as follows: $s(x,t)$ decreases to $s \equiv 0$ and $i(x,t)$ increases to $i \equiv 1$ at about $t = 15$. The populations display monotonic behavior in their time evolutions for fixed $x$ as time $t$ increases, as expected from the SI-model. A comparison of the total populations $S(t)$ and $I(t)$ for $d_s = 10^{-3}$ and $d_i = 10^{-3}$ with the corresponding solutions of the SI system is given in Fig 3.5. In both models, $S(t)$ and $I(t)$ show the same trends, with $S(t)$ decreasing to $S = 0$ and $I(t)$ increasing to $I = 1$ as $t \to \infty$. However, the small diffusivity results in a substantial time delay for equilibration in the values of $S(t)$ and $I(t)$ coming from the diffusive SI model, with $t \approx 15$ for $d_s = 10^{-3}$ and $d_i = 10^{-3}$ as opposed to $t \approx 10$ for $d_s = 10^{-1}$ and $d_i = 1$ seen for regime I. In this regime for the totals, the poor agreement or discrepancies between the diffusive SI model and the SI-model remain throughout, with the largest discrepancies occurring for $d_i = 0$ (no infective diffusion). Clearly in this case, replacing the diffusive SI model by the SI equations (i.e. replacing the integral of a product by the product of the integrals) is no longer permissible.

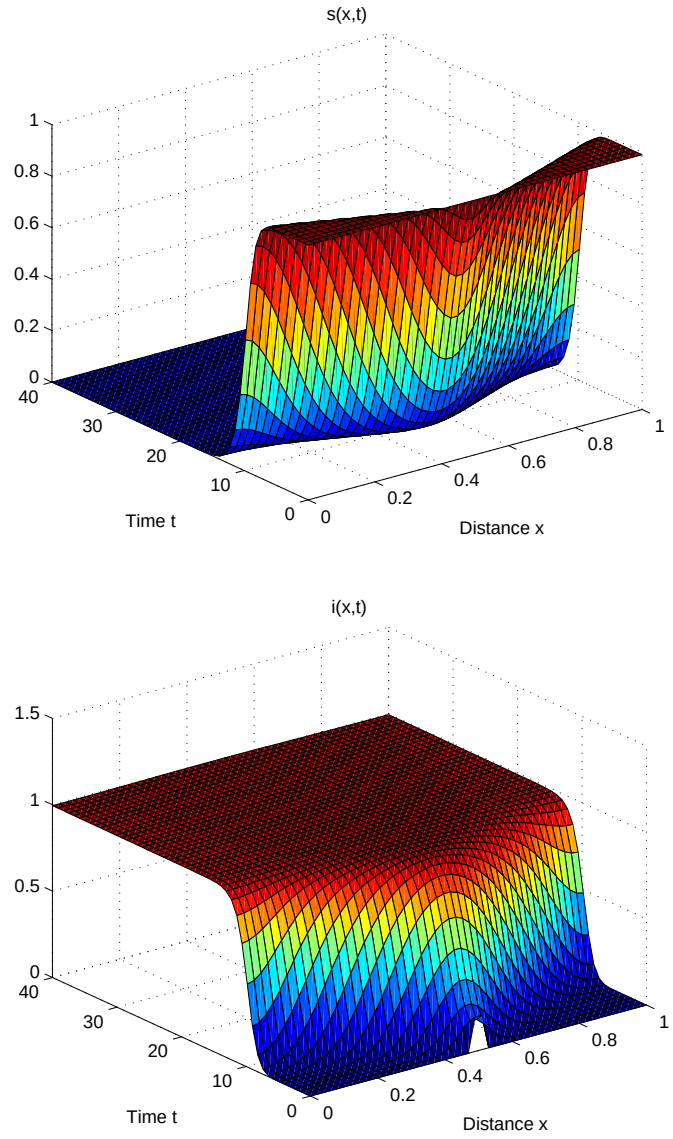


Figure 3.4: Solution of the Diffusive SI model with $d_s = d_i = 0.001$ (regime II: weak SI-diffusion). Both populations $s(x,t)$ and $i(x,t)$ show spatial inhomogeneities up to the equilibration time.

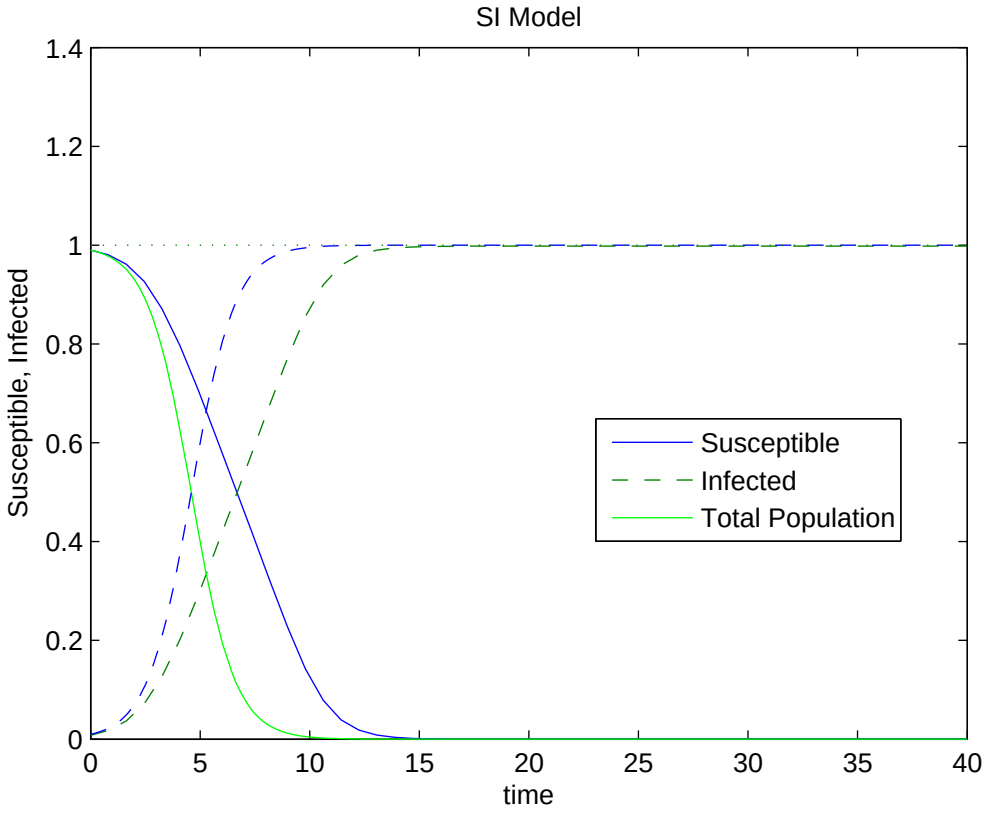


Figure 3.5: Comparison of the totals for the susceptible (S) and infected (I) individuals from the diffusive SI epidemic system when $d_s = d_i = 0.001$ (weak SI-diffusion regime) with the solution of the SI model ($S_0 = 0.99$, $I_0 = 0.01$). The solution of the diffusive SI model lags considerably in time.

## **Regime III** (weak I-diffusion and strong S-diffusion regime)

This regime corresponds to values $d_s \geq 10^{-1}$ and $d_i \leq 10^{-3}$ in the numerical experiments and is characterized by the rapid return to a homogeneous state for the susceptibles and a slow homogenization for the infectives. Furthermore, when $d_i > 0$ we see non-monotonic behavior for the infectives. For a fixed $d_i > 0$, as $d_s$ increases, the susceptibles are redistributed and homogenized faster, but this results in a maintenance of a high rate ($S$) of production of the infectives. This produces a higher peak of infectives near the focus of infection ($x = 1/2$) at the early stage of the process, which slowly subsides. This is shown in Fig 3.5 for diffusivities $d_s = 1$ and $d_i = 10^{-3}$. As time increases both $s(x,t)$ and $i(x,t)$ become spatially homogeneous, with the familiar behavior for the populations occurring, namely $s(x,t)$ going to $s = 0$ and $i(x,t)$ going to $i = 1$, at time $t = 10$. In general, as $d_i$ increases, the behavior of the system starts to resemble regime I. For the totals $S(t)$ and $I(t)$, we have good agreement between the diffusive SI model and the SI-model for $d_s = 1$ and $d_i = 10^{-3}$ as displayed in Fig 3.6 where we see $S(t)$ decaying to $S = 0$ and $I(t)$ growing to $I = 1$ at time $t = 10$. The good agreement between the two models for the totals holds true for all diffusivities in this regime. Therefore, we can say the totals are insensitive to increases in $d_s$ and $d_i$. Consequently, we can replace the PDE system with the ODE system for the diffusivities that lie in this regime.

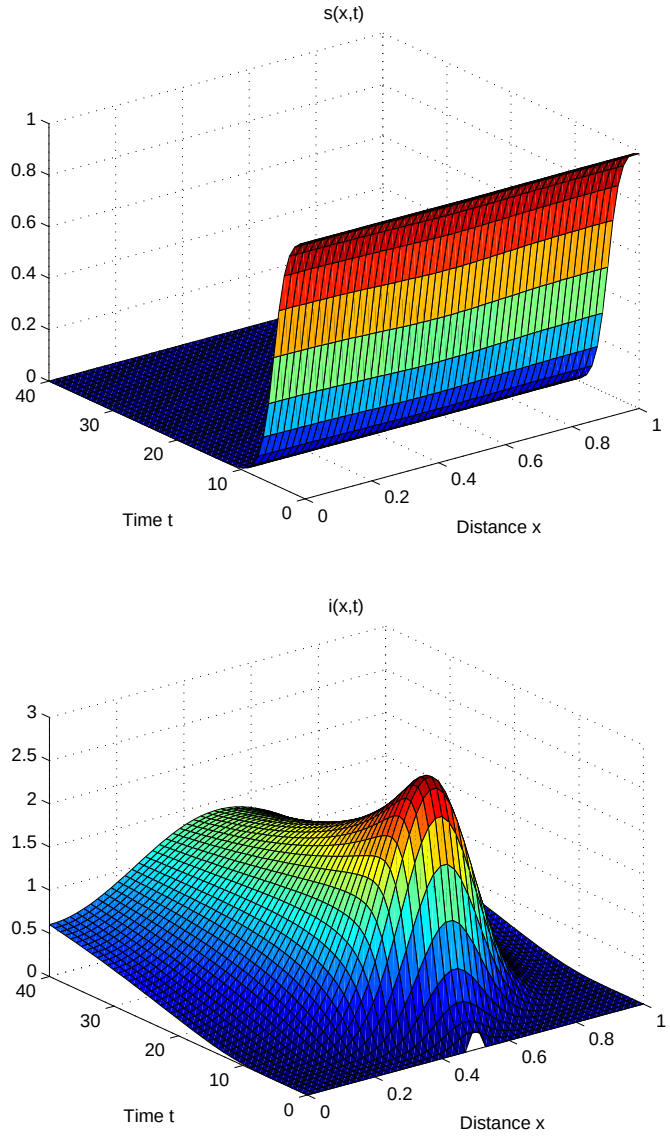


Figure 3.6: Solution of the Diffusive SI model with $d_s = 1$ and $d_i = 0.001$ (regime III: weak I-diffusion and strong S-diffusion). For the populations, $s(x,t)$ becomes spatially homogeneous after a very short time adjustment and $i(x,t)$ shows spatial inhomogeneities.

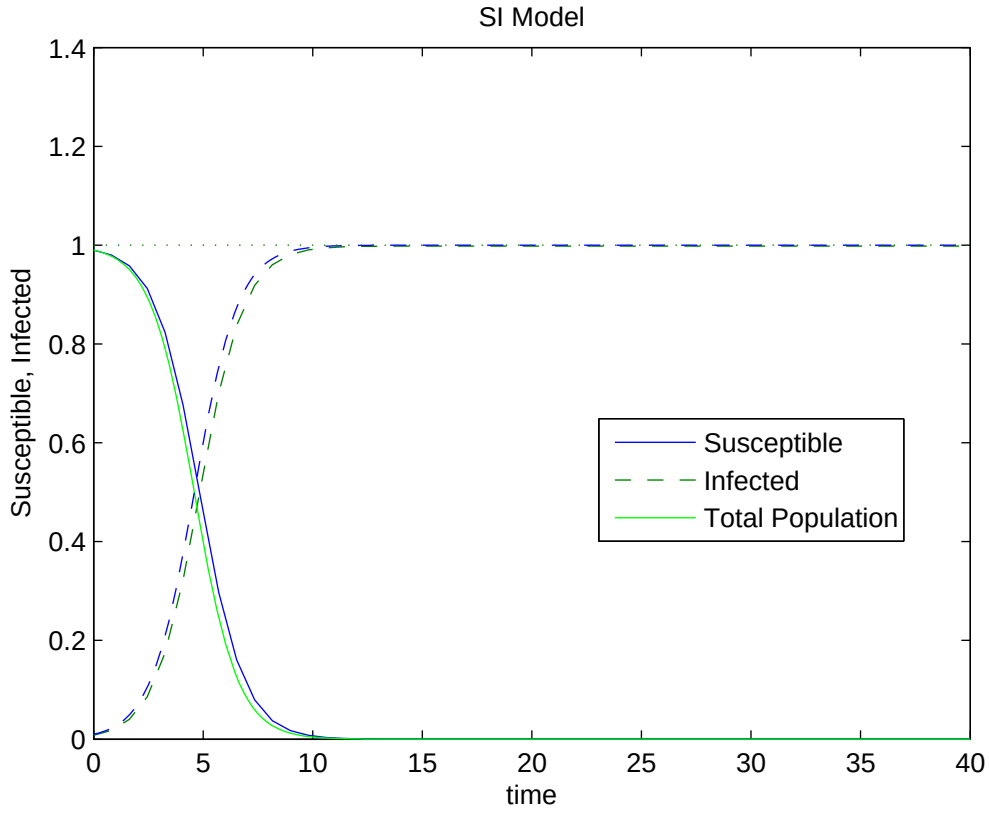


Figure 3.7: Comparison of the totals for the susceptible (S) and infected (I) individuals from the diffusive SI system when $d_s = 1$ and $d_i = 0.001$ (weak I-diffusion and strong S-diffusion regime) with the solution of the SI model ($S_0 = 0.99$, $I_0 = 0.01$). In this case the solution of the diffusive SI model is slightly lagging in time.

# Chapter 4

# Diffusive SIR Model

## 4.1 Introduction

Diffusive models can be extended to include recovered individuals who have the capacity for spatial displacements similar to that of the infected and susceptible individuals in the form of simple diffusion as seen in the previous section leading to what is known as a diffusive SIR model. Diffusive models that include three types of individuals have been studied to a great extent [19],[20],[21],[22]. For example, Murray [21] studied the spread of rabies among foxes with three classes. He proposed the model

$$\begin{aligned} s_t &= as - bs - \frac{(a-b)ns}{K} - \beta rs \\ i_t &= -bi - \frac{(a-b)ni}{K} + \beta rs - \sigma i \\ r_t &= D_r\, r_{xx} - br - \frac{(a-b)nr}{K} + \sigma i - \alpha r \end{aligned} \tag{4.1.1}$$

where only the recovered individuals exhibit movement due to diffusion. Murray

found that the model supports traveling waves with propagation velocity $V$ given by

$$V = (D_r \beta K)^{1/2} v. \tag{4.1.2}$$

Murray also used the parameter values for rabies among foxes given by Anderson [1] to estimate the value propagation velocity $V$ to be

$$V = 51 \text{ km/yr}. \tag{4.1.3}$$

In subsequent work Murray and Seward [22] proposed a three-class reaction-diffusion system to describe the spreading of rabies among foxes,

$$\begin{aligned} s_t &= D_s\, s_{xx} + (a-b)\left(1 - \frac{n}{K}\right) s - \beta r s \\ i_t &= D_i\, i_{xx} + \beta r s - \sigma i - \left[b + (a-b)\frac{n}{K}\right] i \\ r_t &= D_r\, r_{xx} + \sigma i - \alpha r - \left[b + (a-b)\frac{n}{K}\right] r \end{aligned} \tag{4.1.4}$$

where all classes diffuse. Specifically, they were concerned with stopping the spread of rabies among foxes by reducing the number of susceptible foxes below the critical carrying capacity so that the epidemic traveling wave would no longer be sustained. They looked at two methods to reduce the number of susceptible foxes: killing and vaccination. Murray and Seward [22] payed particular attention to the various sizes of regions needed to stop the epidemic traveling wave otherwise known as a break, that is, the area with which you apply the methods to lowering the susceptible foxes, must be large enough to effectively stop the spread of disease (rabies in this case). They conducted many numerical experiments using several diffusivities for Eq.(4.1.14). The diffusion coefficient for the rabid foxes, $D_r$, was fixed and given the value $D_r = 200$ km$^2$ year$^{-1}$. They also set the diffusivities for the susceptible and infected foxes to be equal, $D_s = D_i$, using several values that range from low to high. They concluded that the killing of all classes of foxes is the most effective approach to creating a break, with large breaks needed for high diffusivities.

The previous examples are special cases of the general reaction diffusion system of the form

$$\begin{aligned} s_t &= D_s\, s_{xx} + f(s,i,r) \\ i_t &= D_i\, i_{xx} + g(s,i,r) \\ r_t &= D_r\, r_{xx} + h(s,i,r). \end{aligned} \tag{4.1.5}$$

In this chapter we will consider the diffusive SIR model on a bounded domain

$$\begin{aligned} s_t &= D_s\, s_{xx} - asi \\ i_t &= D_i\, i_{xx} + asi - bi \\ r_t &= D_r\, r_{xx} + bi \end{aligned} \tag{4.1.6}$$

with $0 \leq x \leq L$ and $0 < t < \infty$. Here $s(x,t)$, $i(x,t)$, and $r(x,t)$ represent the density of the susceptible, infected, and recovered class per unit length respectively, $D_s$, $D_i$, $D_r$ are the the diffusion coefficients for the for the susceptible, infected, and recovered class, and $a$ is a measure of the virulence strength of the disease and $b$ is the removal rate.

The diffusive SIR system is supplemented with Neumann boundary conditions at both ends,

$$s_x(0,t) = 0 \qquad \text{and} \qquad s_x(L,t) = 0 \tag{4.1.7}$$

$$i_x(0,t) = 0 \qquad \text{and} \qquad i_x(L,t) = 0 \tag{4.1.8}$$

$$r_x(0,t) = 0 \qquad \text{and} \qquad r_x(L,t) = 0 \tag{4.1.9}$$

and with initial conditions

$$s(x,0) = s_0(x) \geq 0, \qquad i(x,0) = i_0(x) \geq 0 \qquad \text{and} \qquad r(x,0) = r_0(x) \geq 0. \tag{4.1.10}$$

Associated with the densities $s(x,t)$, $i(x,t)$, and $r(x,t)$ are the total number of susceptible $S(t)$, the total number of infected $I(t)$, the total number of recovered $R(t)$ and the total number of individuals that make up the population $N(t)$, defined by

$$\begin{aligned} S(t) &= \int_0^L s(x,t)\,dx \\ I(t) &= \int_0^L i(x,t)\,dx \\ R(t) &= \int_0^L r(x,t)\,dx \\ N(t) &= S(t) + I(t) + R(t). \end{aligned} \tag{4.1.11}$$

From this we can prove that $N(t)$ is a conserved quantity for the diffusive SIR system with Neumann boundary conditions,

$$\begin{aligned} \frac{dN}{dt} &= \frac{dS}{dt} + \frac{dI}{dt} + \frac{dR}{dt} \\ &= \int_0^L s_t\,dx + \int_0^L i_t\,dx + \int_0^L r_t\,dx \\ &= \int_0^L (D_s\, s_{xx} - asi)\,dx + \int_0^L (D_i\, i_{xx} + asi - bi)\,dx + \int_0^L (D_r\, r_{xx} + bi)\,dx \\ &= D_s\, s_x\Big|_0^L + D_i\, i_x\Big|_0^L + D_r\, r_x\Big|_0^L - \int_0^L asi\,dx + \int_0^L asi - bi\,dx + \int_0^L bi\,dx \\ &= 0, \end{aligned}$$

because of the zero flux boundary conditions, and we conclude that

$$N(t) \equiv N(0) = N_0 \tag{4.1.12}$$

for all times, where $N_0 = S_0 + I_0 + R_0$ is the total initial population. In particular, it follows that $S$, $I$ and $R$ are bounded by $N_0$ from above and $N$ is conserved.

If the initial data is spatially homogeneous, $s(x,0) = s_0$, $i(x,0) = i_0$, then the diffusive SIR model admits a spatially homogeneous solution $s(x,t) = s(t)$, $i(x,t) = i(t)$, and $r(x,t) = r(t)$. Moreover, in this case the integrated values of $s(t)$, $i(t)$, and $r(t)$ in Eq.(4.1.1) become

$$S(t) = Ls(t) \tag{4.1.13}$$

$$I(t) = Li(t) \tag{4.1.14}$$

$$R(t) = Lr(t) \tag{4.1.15}$$

and they solve the SIR ODE system studied in Chapter 2, namely

$$\begin{aligned} \frac{dS}{dt} &= -\alpha SI, \qquad S(0) = Ls_0 \\ \frac{dI}{dt} &= \alpha SI - bI, \qquad I(0) = Li_0 \\ \frac{dR}{dt} &= bI, \qquad R(0) = Lr_0 \end{aligned} \tag{4.1.16}$$

with $\alpha = (a/L)$. Now, the threshold criterion given in Chapter 2 for the development of an epidemic in the SIR model is given by

$$S_0 > \frac{b}{\alpha} = \frac{bL}{a}$$

and recalling that from Eq.(4.1.12) that $S_0 = s_0 L$ we arrive at

$$s_0 > \frac{b}{a}. \tag{4.1.17}$$

Evidently this corresponds to the criticality criterion $S_0 > c = (b/aN_0)$ obtained in Chapter 2 and quantifies the outbreak of epidemic depending on whether $aS_0$, the product of the virulence strength and the initial population density of susceptibles, is larger or smaller than $b$, the rate of recovery of the infected.

Next we simplify Eq.(4.1.1) by non-dimensionalization of the system. To do so we introduce the non-dimensional variables

$$\widetilde{s} = \frac{sL}{N_0}, \quad \widetilde{i} = \frac{iL}{N_0}, \quad \widetilde{r} = \frac{rL}{N_0}, \quad \widetilde{t} = \frac{aN_0\, t}{L}, \quad \widetilde{x} = \frac{x}{L} \tag{4.1.18}$$

where $N_0 = S_0 + I_0 + R_0$. If we define

$$\widetilde{S}(t) = \frac{S(t)}{N_0}, \quad \widetilde{I}(t) = \frac{I(t)}{N_0}, \quad \widetilde{R}(t) = \frac{R(t)}{N_0}, \quad \widetilde{N}(t) = \frac{N(t)}{N_0} \tag{4.1.19}$$

where $S(t)$, $I(t)$, $R(t)$, and $N(t)$ are given in Eq.(4.1.6), then it follows from Eq.(4.1.13) that

$$\widetilde{N}(t) = \frac{N(t)}{N_0} \equiv 1. \tag{4.1.20}$$

Next we introduce the non-dimensional variables for Eq.(4.2.7) into Eq.(4.2.1)

$$a\left(\frac{N_0}{L}\right)^2 \frac{\partial \tilde{s}}{\partial \tilde{t}} = D_s \frac{N_0}{L^3} \frac{\partial^2 \tilde{s}}{\partial \tilde{x}^2} - a\left(\frac{N_0}{L}\right)^2 \tilde{s}\tilde{i} \tag{4.1.21}$$

$$a\left(\frac{N_0}{L}\right)^2 \frac{\partial \tilde{i}}{\partial \tilde{t}} = D_i \frac{N_0}{L^3} \frac{\partial^2 \tilde{i}}{\partial \tilde{x}^2} + a\left(\frac{N_0}{L}\right)^2 \tilde{s}\tilde{i} - b\left(\frac{N_0}{L}\right) \tilde{i} \tag{4.1.22}$$

$$a\left(\frac{N_0}{L}\right)^2 \frac{\partial \tilde{r}}{\partial \tilde{t}} = D_r \frac{N_0}{L^3} \frac{\partial^2 \tilde{r}}{\partial \tilde{x}^2} + b\left(\frac{N_0}{L}\right) \tilde{i}$$

If we drop the tildes for notational simplicity and let $c = (bL/aN_0)$ then we arrive at the **non-dimensionalized diffusive SIR model**

$$\begin{aligned} s_t &= d_s\, s_{xx} - si \\ i_t &= d_i\, i_{xx} + si - ci \\ r_t &= d_r\, r_{xx} + ci \end{aligned} \tag{4.1.23}$$

where $d_s = (D_s/aN_0L)$, $d_i = (D_i/aN_0L)$, and $d_r = (D_r/aN_0L)$ are the non-dimensional diffusivities. The initial data given by

$$s(x,0) = s_0(x) \geq 0, \qquad i(x,0) = i_0(x) \geq 0 \quad \text{and} \quad r(x,0) = r_0(x) \geq 0 \tag{4.1.24}$$

with $0 \leq x \leq 1$. Finally we impose Neumann boundary conditions at the endpoints $x = 0, 1$

$$\begin{aligned} s_x(x,t)|_{x=0,1} &= 0 \\ i_x(x,t)|_{x=0,1} &= 0 \\ r_x(x,t)|_{x=0,1} &= 0. \end{aligned} \tag{4.1.25}$$

With the above choices of scales the total population becomes normalized to the value one

$$N(t) = \int_0^1 s(x,t)\, dx + \int_0^1 i(x,t)\, dx + \int_0^1 r(x,t)\, dx \equiv N_0 \equiv 1. \tag{4.1.26}$$

In the next two sections we are going to study the diffusive SIR system, Eqs.(4.1.23-25), paying special attention to the effects that the spatial diffusivities $d_s$, $d_i$, $d_r$ and the criticality condition, Eq.(4.1.17), have on the propagation of the infectious disease. In section 4.2 we will study the diffusive SIR model with supercritical (epidemic outbreak) initial conditions, $s_0 > c$, and in section 4.3 we will turn the attention to subcritical (no epidemic outbreak) initial conditions, $s_0 < c$. In these studies we always assume that susceptible and recovered exhibit the same type of mobility, that is, the diffusivities $d_s$ and $d_r$ are equal, $d_s = d_r$. On the other hand, these are reasons to believe that infection can affect mobility of the individuals, so we will consider both cases where $d_i = d_s = d_r$ and $d_i \neq d_s = d_r$.

Regarding the initial conditions, we assume that $s(x,0)$ and $i(x,0)$ are described by Gaussian distributions centered at $x = 1/2$; $s(x,0)$ is given by a broad Gaussian

($\sigma_1 = 100$)

$$s(x,0) = s_0 \, \frac{e^{-\sigma_1 (x-1/2)^2}}{\displaystyle\int_0^1 e^{-\sigma_1 (x-1/2)^2} \, dx} = s_0 \, g_1(x) \quad \text{with} \quad \sigma_1 = 100 \tag{4.1.27}$$

and $i(x,0)$ is given by a centralized Gaussian ($\sigma_2 = 10,000$)

$$i(x,0) = i_0 \, \frac{e^{-\sigma_2 (x-1/2)^2}}{\displaystyle\int_0^1 e^{-\sigma_2 (x-1/2)^2} \, dx} = i_0 \, g_2(x) \quad \text{with} \quad \sigma_2 = 10,000. \tag{4.1.28}$$

Finally, we assume zero initial population $r(x,0)$ for the recovered class,

$$r(x,0) = r_0 = 0. \tag{4.1.29}$$

From Eq.(4.1.27) (and hence for Eq.(4.1.28)) it follows that the contribution from the tail of the Gaussian is very small, in fact,

$$\int_{-\infty}^{\infty} e^{-\sigma_1 (x-1/2)^2} \, dx - \int_0^1 e^{-\sigma_1 (x-1/2)^2} \, dx \cong 0.00001, \tag{4.1.30}$$

so that the initial distributions can be viewed as Gaussians over all space. A plot of these normalized Gaussian functions $g_1(x)$, $g_2(x)$, centered at $x = 1/2$,

$$g_1(x) = \frac{e^{-\sigma_1 (x-1/2)^2}}{\displaystyle\int_0^1 e^{-\sigma_1 (x-1/2)^2} \, dx} \tag{4.1.31}$$

$$g_2(x) = \frac{e^{-\sigma_2 (x-1/2)^2}}{\displaystyle\int_0^1 e^{-\sigma_2 (x-1/2)^2} \, dx} \tag{4.1.32}$$

for $\sigma_1 = 100$ and $\sigma_2 = 10,000$ is given in Fig 4.1. Clearly the infected class is highly concentrated around the centralized area $x = 1/2$, whereas the susceptible class has a substantially larger geographical spreading.

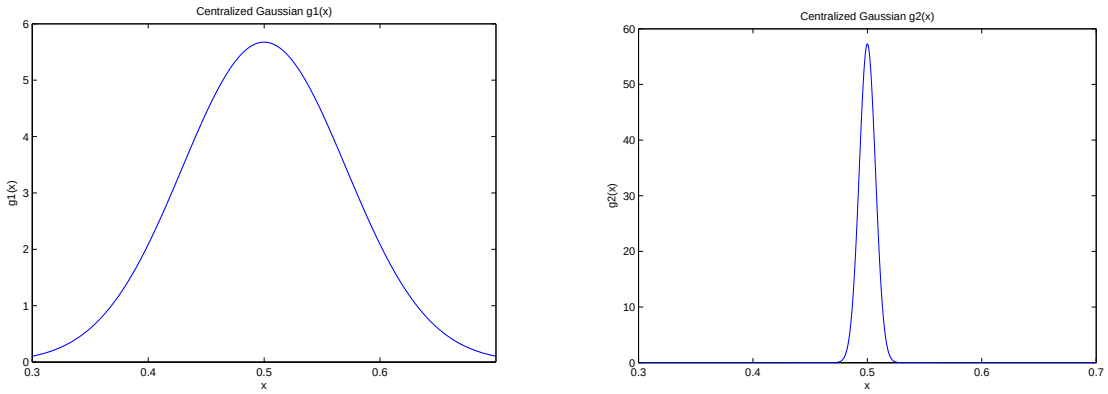


Figure 4.1: Plot of the Normalized Gaussians centered at $x = 1/2$ given by Eqs.(4.3.31-32). The function $g_1(x)$ is centered around $x = 1/2$ and concentrated around this point. The function $g_2(x)$ is concentrated almost entirely around $x = 1/2$.

Finally, since the total initial population is given by

$$\int_0^1 s(x,0)\, dx = \int_0^1 s_0\, g_1(x)\, dx = s_0,$$

then the criticality condition for the epidemic is given by $s_0 > c$.

In the next two sections we look at the diffusive SIR system for both equal and unequal diffusivities, where we divide these sections according to the supercritical and subcritical cases $s_0 > c$ and $s_0 < c$ seen for epidemic growth or hindrance in the SIR model. For comparison between the diffusive SIR model and the SIR model of Chapter 2, we choose the same values for the initial populations, $s_0$, $i_0$, $r_0$ and the same value for $c$ for the present model. The totals for these initial populations correspond to $S_0$, $I_0$ and $R_0$ and are the same as their counterparts in the SIR model. We will employ the same numerical procedure developed in the previous chapter to determine the characteristics and qualitative behavior of the populations. In addition, we will compare the the diffusive SIR model with the SIR model by explicitly looking at the total values $S(t)$, $I(t)$ and $R(t)$ for both models.

## 4.2 Diffusive SIR Model with Equal and Non-Equal Diffusivities with $s_0 > c$

In this section we study the diffusive SIR model for both equal and unequal diffusivities, i.e. $d_s = d_r = d_i$ and $d_s = d_r \neq d_i$, respectively, and with the supercritical case $s_0 > c$. For comparison with the SIR model of Chapter 2, we select the same values for the initial populations. For all experiments we have $s_0 = 0.99$ (99% susceptible population), $i_0 = 0.01$ (1% infected population), $r_0 = 0$ (no recovered) and $c = 0.5$, so that $s_0 > c$. We performed a series of numerical experiments covering a wide range of the diffusion coefficients. Specifically, we considered diffusion coefficients with values $d_i, d_s = d_r = 0, 10^{-3}, 10^{-2}, 10^{-1}, 10^{0}, 10^{1}$ spanning five orders of magnitude in parameter space, and including the ranges of strong and weak diffusivities for the susceptible, infected and recovered populations. There values of the diffusivities are collected in Table 4.1.

In Table 4.1 we identified four regimes in parameter space for which the solutions of the diffusive SIR equations display similar qualitative behavior. This behavior is dictated in great measure by the relative strength of the diffusion in the infected population (I-diffusion) over the susceptible and recovered populations (SR-diffusion). Regime I corresponds to strong SIR-diffusion. Regime II corresponds to strong I-diffusion and weak SR-diffusion. Regime III corresponds to weak I-diffusion and strong SR-diffusion. Finally, Regime IV corresponds to weak SIR-diffusion.

Table 4.1: Diffusivity values for the susceptible, infected and recovered individuals that are categorized into four unique solutions depending on the various pairings of these values.

| $d_i \backslash^{d_s=d_r}$ | 0 | 0.001 | 0.01 | 0.1 | 1 | 10 |
|---|---|---|---|---|---|---|
| 0 | *IV* | *IV* | *IV* | *III* | *III* | *III* |
| 0.001 | *IV* | *IV* | *IV* | *III* | *III* | *III* |
| 0.01 | *IV* | *IV* | *IV* | *I* | *I* | *I* |
| 0.1 | *IV* | *IV* | *IV* | *I* | *I* | *I* |
| 1 | *II* | *II* | *II* | *I* | *I* | *I* |
| 10 | *II* | *II* | *II* | *I* | *I* | *I* |

## **Regime I** (strong SIR-diffusion regime)

This regime corresponds to values of $d_s = d_r \geq 10^{-1}$ and $d_i \geq 1$ in the numerical experiments. It is characterized by the rapid homogenization of the susceptible, infected and recovered individuals. Due to strong diffusivities, after a short time interval, the initially inhomogeneous susceptible and infected spread out quickly, leading to solutions that are constant in space (spatially inhomogeneous) for all populations. This is demonstrated in Fig 4.2, which displays the susceptible, infected and recovered for $d_s = d_r = 1$ and $d_i = 10^{-1}$. For the populations, $s(x,t)$, $i(x,t)$ and $r(x,t)$ become spatially homogeneous, with $s(x,t)$ decreasing to $s \approx 0.2$, $i(x,t)$ increasing to a maximum value $i \approx 0.15$ and then decreasing to a minimum value $i = 0$ and $r(x,t)$ increasing to $r \approx 0.8$. Now, a comparison between the SIR model and the diffusive SIR model yields good agreement between the models with the solutions of the total populations $S(t)$, $I(t)$ and $R(t)$ tending towards equilibrium in the same fashion. This is shown in Fig 4.3, with the unconnected lines representing the diffusive SIR model and the connected lines representing the SIR model, $S(t)$ goes to $S = 0.2$ (20% susceptible population), $I(t)$ initially grows to $I = 0.15$ then decays to $I = 0$ (no infected), and $R(t)$ increases to $R \approx 0.8$ (80% recovered population). We also see essentially no difference between the time in which equilibration is reached for the diffusive SIR model and the SIR-model, which does so at $t = 25$. In this regime the diffusivities are high enough to permit the replacement of the diffusive SIR model by the simpler SIR model.

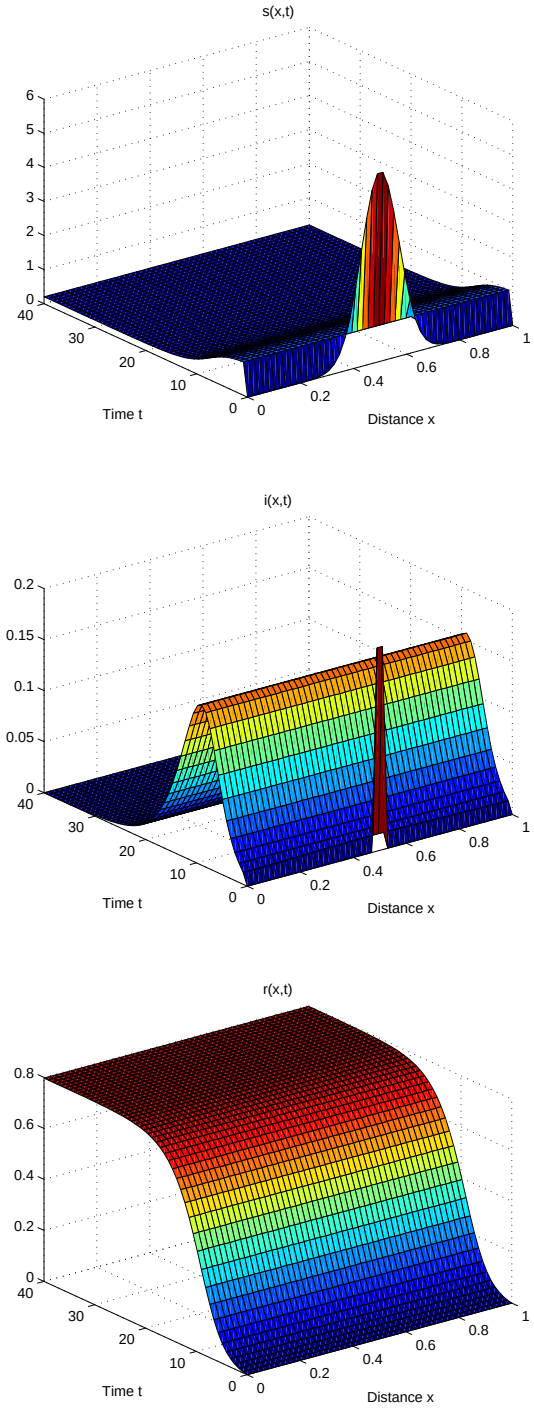


Figure 4.2: Solution of the Diffusive SIR model with $d_s = d_r = 1$ and $d_i = 0.1$ (regime I: strong SIR-diffusion). For the populations, $s(x,t)$, $i(x,t)$ and $r(x,t)$ become spatially homogeneous after a very short adjustment time.

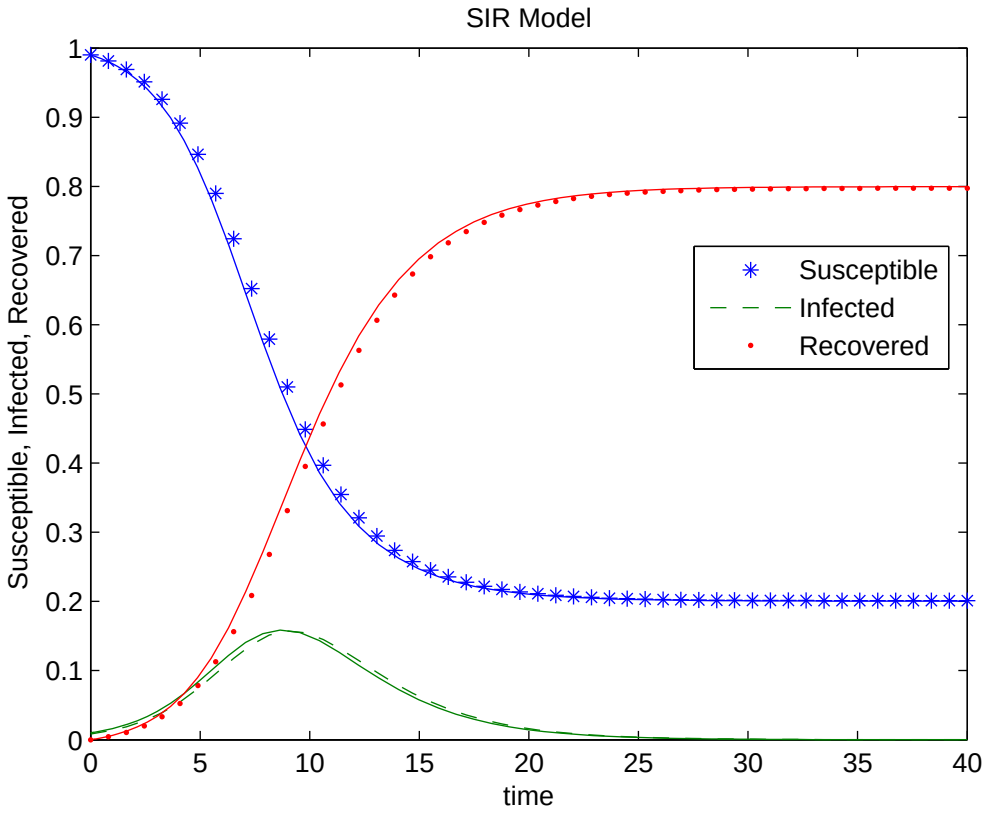


Figure 4.3: Comparison of the totals for the susceptible (S), infected (I) and recovered (R) individuals from the diffusive SIR system when $d_s = d_r = 1$ and $d_i = 0.1$ (strong SIR-diffusion regime) with the solution of the SIR model ($S_0 = 0.99$, $I_0 = 0.01$ and $R_0$=0) with $c = 0.5$. In this case no time lag in the solution of the diffusive SIR model.

## **Regime II:** (strong I-diffusion and weak SR-diffusion regime)

This regime corresponds to values $d_s = d_r \leq 10^{-2}$ and $d_i \geq 1$ in the numerical experiments. A representative solution is given in Fig 4.4 which shows the time evolutions for the susceptible, infected and recovered individuals for $d_s = d_r = 10^{-3}$ and $d_i = 1$. We see slow homogenization of the susceptibles and recovered and rapid homogenization for the infectives. The final fate for all individuals is identical to that of the strong SIR-diffusion regime, namely the homogeneous progression is as follows: $s(x,t)$ decaying to a minimum value $s \approx 0.2$, $i(x,t)$ initially increasing to a maximum value and then decreasing to a minimum value $i = 0$, and $r(x,t)$ growing to maximum value $r \approx 0.8$. Therefore we can assume that the value for the totals $S(t)$, $I(t)$ and $R(t)$ are exactly like the totals for the previous regime. This is accurate as we see in Fig 4.5 for the diffusion coefficient values $d_s = d_r = 10^{-3}$ and $d_i = 1$ . Once again we have $S(t)$ going to $S = 0.2$ (20% susceptible population), $I(t)$ initially growing to $I = 0.15$ then decaying to $I = 0$ (no infected), and $R(t)$ increasing to $R \approx 0.8$ (80% recovered population) at time $t = 25$. We have good agreement between the diffusive SIR model and the SIR model. Consequently we can replace the more complicated diffusive SIR system with the simpler SIR system.

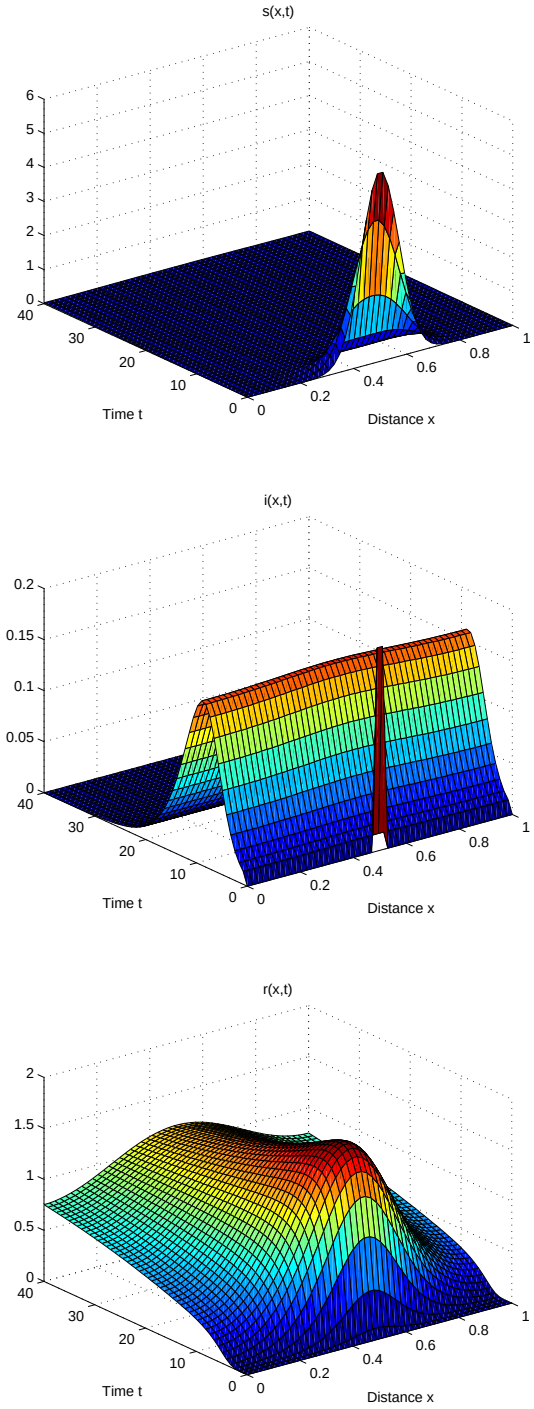


Figure 4.4: Solution of the Diffusive SIR model with $d_s = d_r = 0.001$ and $d_i = 1$ (regime II: strong I-diffusion and weak SR-diffusion). For the populations, $s(x,t)$ and $r(x,t)$ show spatial inhomogeneity until equilibrium is reached, $i(x,t)$ becomes spatially homogeneous after a very short adjustment time.

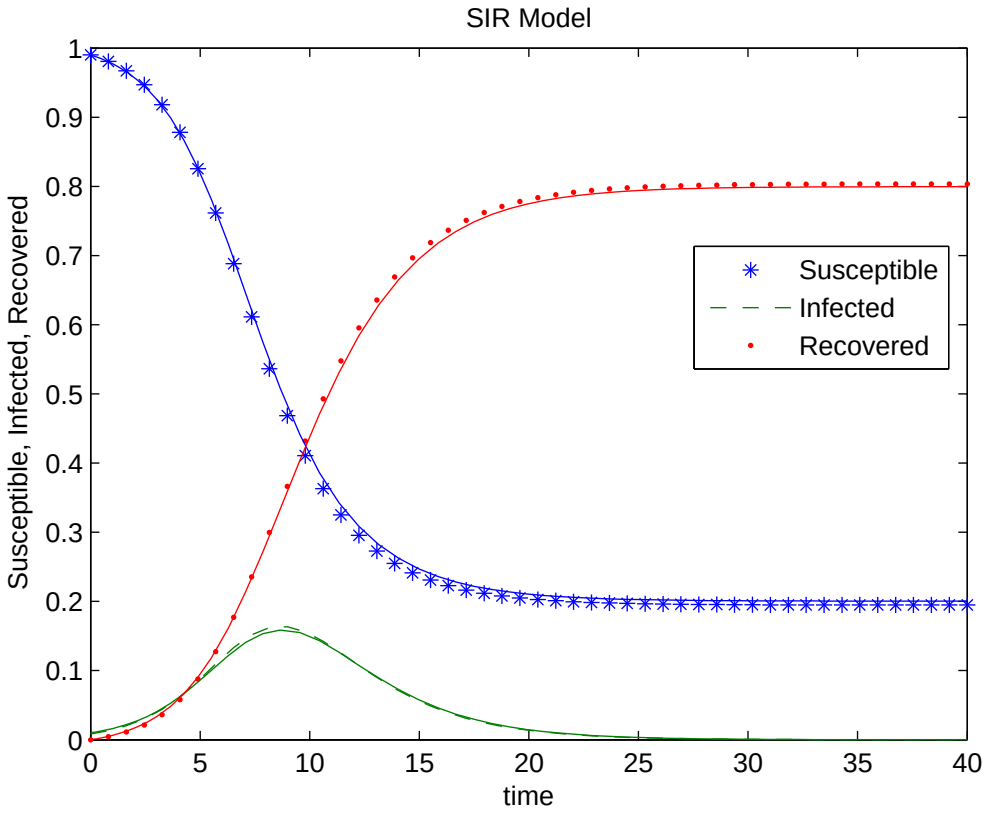


Figure 4.5: Comparison of the totals for the susceptible (S), infected (I) and recovered (R) individuals from the diffusive SIR epidemic system when $d_s = d_r = 0.001$ and $d_i = 1$ (strong I-diffusion and weak SR-diffusion regime) with the solution of the SIR model ($S_0 = 0.99$, $I_0 = 0.01$ and $R_0 = 0$). The solution of the diffusive SIR model equilibrates at the same rate.

## **Regime III:** (weak I-diffusion and strong SR-diffusion regime)

This regime corresponds to values $d_s = d_r \geq 10^{-1}$ and $d_i \leq 10^{-3}$ in the numerical experiments. It is characterized by rapid homogenization of both the susceptible and recovered individuals and the slow homogenization of the infected individuals. Additionally, we have non-monotonic behavior for the infectives. The presence of strong diffusivity leads to the initially in-homogeneous susceptible population dispersing quickly and therefore causing the rapid homogenization of both the susceptible and recovered individuals and the reaction mechanism causes the non-monotonic behavior for the infected population which decreases with time. In Fig 4.6 this is clearly demonstrated, with the susceptible, infected, and recovered populations displayed for $d_s = d_r = 1$ and $d_i = 10^{-3}$. Eventually, the in-homogeneities for the infectives subside, due to their transition into the recovered population. So we have $s(x,t)$, $i(x,t)$ and $r(x,t)$ becoming spatially homogeneous, with $s(x,t)$ decaying to $s \approx 0.2$, $i(x,t)$ growing to maximum value then decaying to $i = 0$ and $r(x,t)$ growing to $r \approx 0.8$ at time $t = 25$. As we have seen, for these final values of the individuals we should expect good agreement between the total populations, $S(t)$, $I(t)$ and $R(t)$ for the diffusive SIR model and their counterparts for the SIR model. In Fig 4.7 we see that this is indeed the case, with essentially no difference for when equilibrium is reached. In spite of the spatial inhomogeneities, we can safely replace the diffusive SIR model by the simpler SIR model.

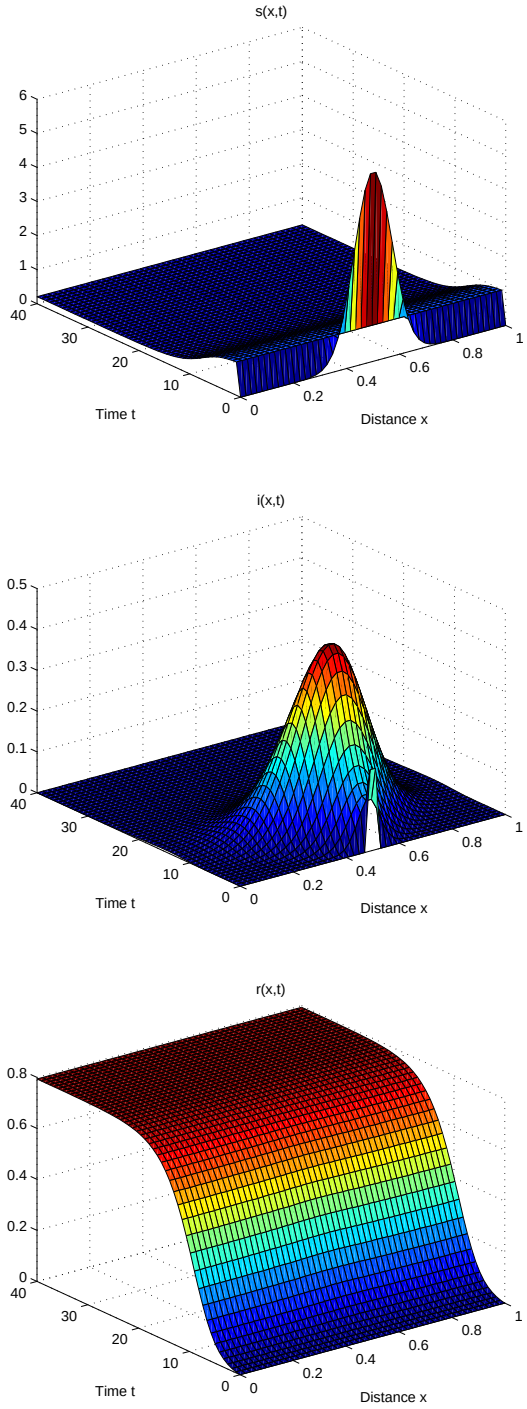


Figure 4.6: Solution of the Diffusive SIR model with $d_s = d_r = 1$ and $d_i = 0.001$ (regime III: weak I-diffusion and strong SR-diffusion). For the populations, $s(x,t)$ and $r(x,t)$ become spatially homogeneous after a very short adjustment time and $i(x,t)$ shows spatial inhomogeneity until equilibrium is reached.

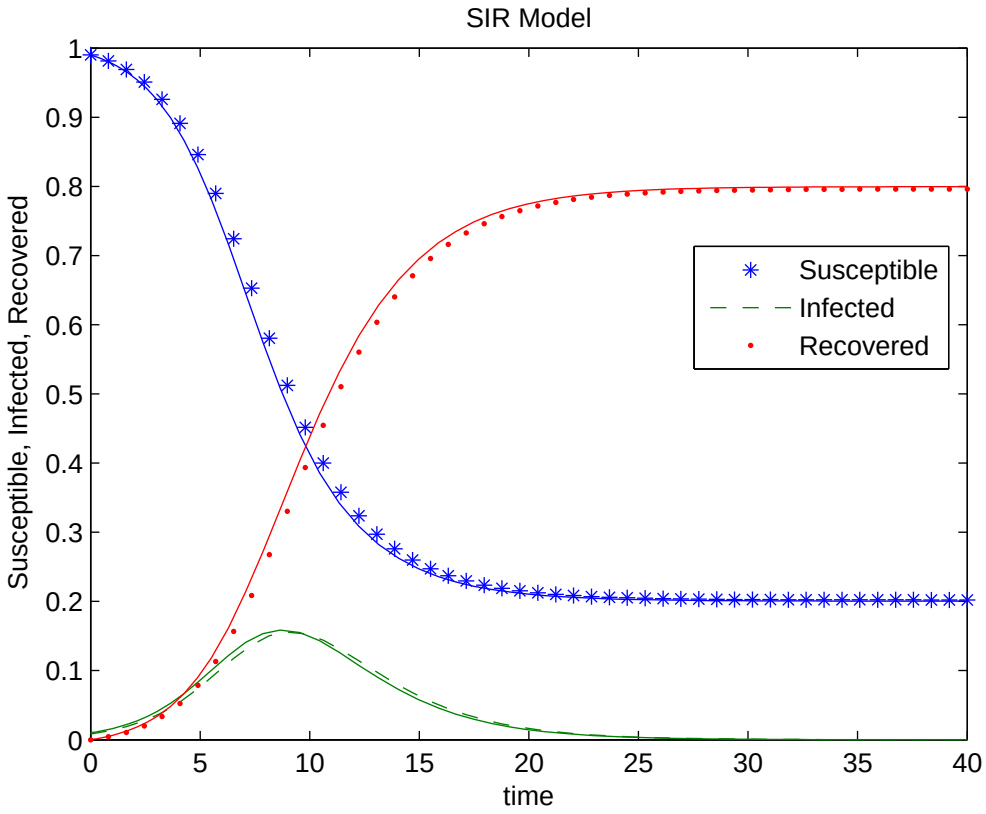


Figure 4.7: Comparison of the totals for the susceptible (S), infected (I) and recovered (R) individuals from the diffusive SIR epidemic system when $d_s = d_r = 1$ and $d_i = 0.001$ (weak I-diffusion and strong SR-diffusion regime) with the solution of the SIR model ($S_0 = 0.99$, $I_0 = 0.01$ and $R_0 = 0$). The solution of the diffusive SIR model equilibrates at the same rate.

## **Regime IV:** (weak SIR-diffusion regime)

This regime corresponds to values $d_s = d_r \leq 10^{-2}$ and $d_i \leq 10^{-1}$ in the numerical experiments. It is characterized by the slow homogenization of the susceptible, infected and recovered populations. We also have non-monotonic behavior for the infectives and persistence of spatial structures for the recovered. A representative solution is given in Fig 4.8 which shows the time evolutions for the susceptible, infected and recovered individuals for $d_s = d_r = 10^{-3}$ and $d_r = 10^{-2}$. The final fate for all individuals is of a homogeneous progression with $s(x,t)$ decaying to $s \approx 0.05$, $i(x,t)$ initially increasing to a maximum value and then decreasing to a minimum value $i = 0$, and $r(x,t)$ growing to $r \approx 0.95$. When compared to the previous regimes we see differences in the asymptotic states of the populations. We have more of the population becoming infected and therefore have less susceptible and more recovered. This difference will obviously be reflected in the totals for the populations, where we expect to have disagreements between the SIR model and the diffusive SIR model. This is indeed the case, as shown in Fig 4.9, with $S(t)$ going to $S = 0.05$ (5% susceptible population), $I(t)$ going to $I = 0$ (no infected) and $R(t)$ going to $R = 0.95$ (95% recovered population) as $t \to \infty$. For these values we also have equilibration being reached faster in the diffusive SIR model, with $t = 15$ for $d_s = d_r = 10^{-3}$ and $d_r = 10^{-2}$ as contrasted with $t = 25$ for the SIR model. Clearly we have marked disagreements in the predictions from both models, with more infectives, less susceptibles and much more recovered for the diffusive SIR model.

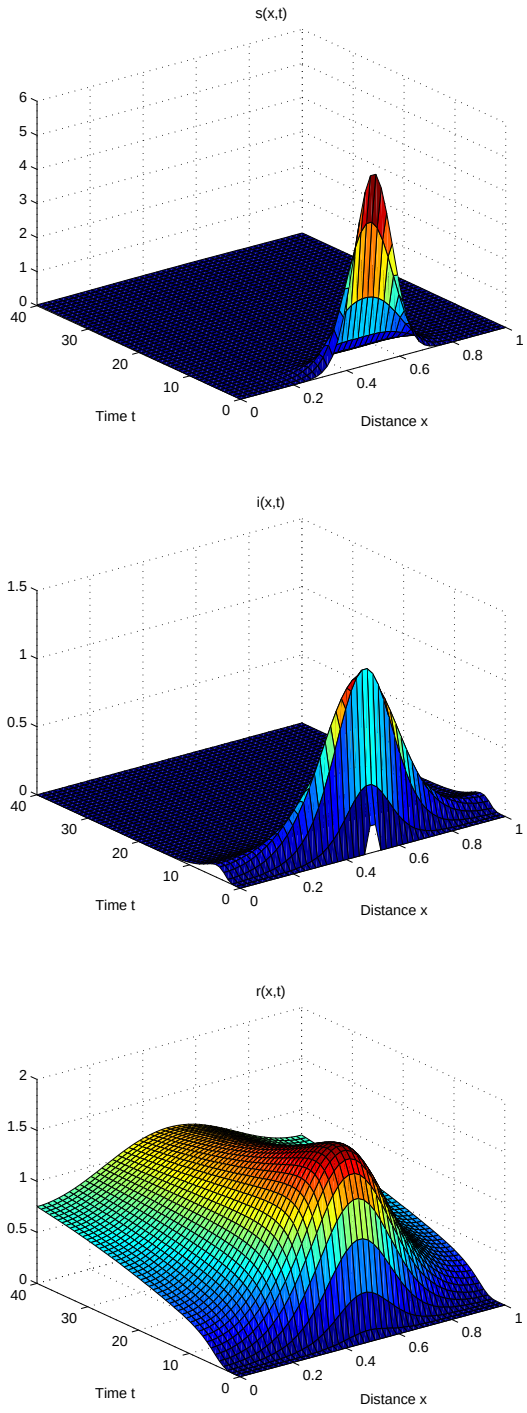


Figure 4.8: Solution of the Diffusive SIR model with $d_s = d_r = 0.01$ and $d_i = 0.001$ (regime IV: weak SIR-diffusion). For the populations, $s(x,t)$, $i(x,t)$ and $r(x,t)$ show spatial inhomogeneities until the equilibrium time.

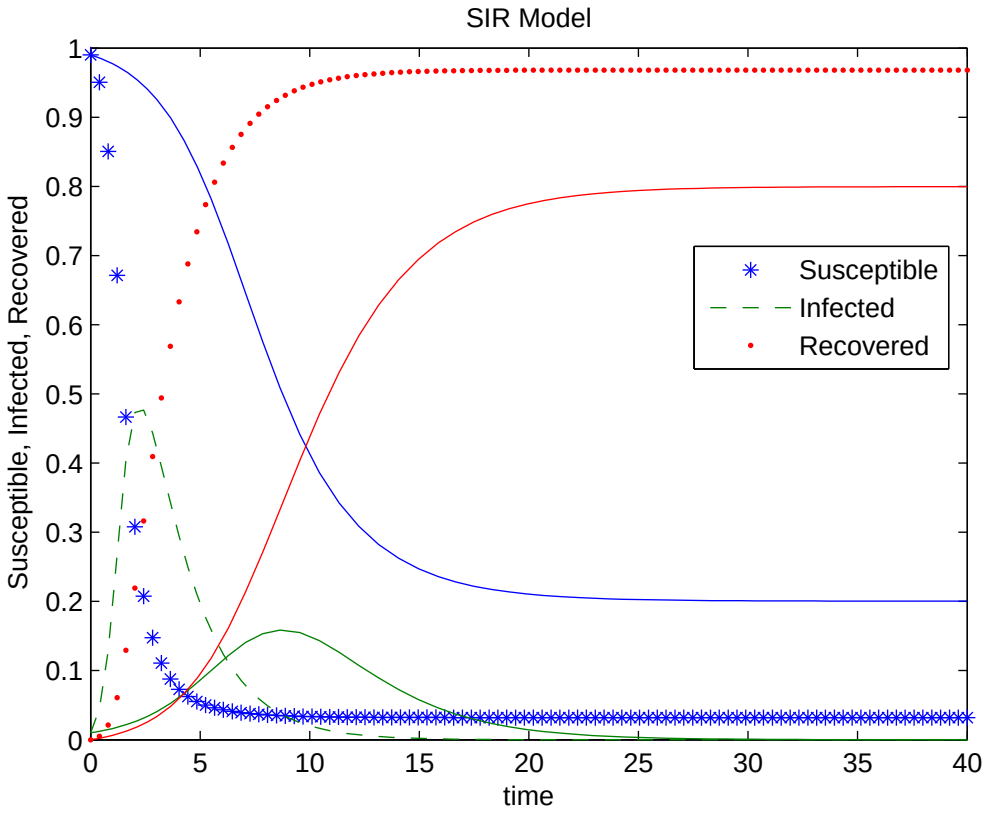


Figure 4.9: Comparison of the totals for the susceptible (S), infected (I) and recovered (R) individuals from the diffusive SIR epidemic system when $d_s = d_r = 0.01$ and $d_i = 0.001$ (weak SIR-diffusion regime) with the solution of the SIR model ($S_0 = 0.99$, $I_0 = 0.01$ and $R_0 = 0$). The solution of the diffusive SIR model equilibrates at a faster rate.

## 4.3 Diffusive SIR Model with Equal and Non-Equal Diffusivities with $s_0 < c$

In this section we study the diffusive SIR model for both equal and unequal diffusivities, i.e. $d_s = d_r = d_i$ and $d_s = d_r \neq d_i$, respectively, and under the subcritical initial condition, $s_0 < c$. To contrast with the SIR model of Chapter 2, we use the same values for the initial populations. For all experiments we have $s_0 = 0.4$ (40% susceptible population), $i_0 = 0.6$ (60% infected population), $r_0 = 0$ (no recovered) and $c = 0.5$, so that $s_0 < c$. We carried out many numerical experiments spanning a large range of diffusion coefficients. In particular, we considered diffusion coefficients with values $d_i, d_s = d_r = 0, 10^{-3}, 10^{-2}, 10^{-1}, 10^{0}, 10^{1}$ spanning five orders of magnitude in parameter space, and encompassing strong and weak diffusivities for the susceptible, infected and recovered populations. There values of the diffusivities are gathered in Table 4.2.

In Table 4.2 we recognized four regimes in parameter space for which the solutions of the diffusive SIR equations show much of the same behavior. This behavior is created in large part by the relative strength of the diffusion in the infected population (I-diffusion) over the susceptible and recovered populations (SR-diffusion). Regime I corresponds to strong SIR-diffusion. Regime II corresponds to strong I-diffusion and weak SR-diffusion. Regime III corresponds to weak I-diffusion and strong SR-diffusion. Finally, Regime IV corresponds to weak SIR-diffusion.

Table 4.2: Diffusivity values for the susceptible, infected, and recovered individuals that are categorized into one of four solutions depending on the various pairings of these values.

| $d_i \backslash^{d_s=d_r}$ | 0 | 0.001 | 0.01 | 0.1 | 1 | 10 |
|---|---|---|---|---|---|---|
| 0 | *IV* | *IV* | *IV* | *III* | *III* | *III* |
| 0.001 | *IV* | *IV* | *IV* | *III* | *III* | *III* |
| 0.01 | *IV* | *IV* | *IV* | *I* | *I* | *I* |
| 0.1 | *IV* | *IV* | *IV* | *I* | *I* | *I* |
| 1 | *II* | *II* | *II* | *I* | *I* | *I* |
| 10 | *II* | *II* | *II* | *I* | *I* | *I* |

## **Regime I:** (strong SIR-diffusion regime)

This regime corresponds to values $d_s = d_r \geq 10^{-1}$ and $d_i \geq 10^{-2}$ in the numerical experiments. It is characterized by the rapid homogenization of all populations. In Fig 4.10 this is clearly demonstrated for $d_s = d_r = 10^{-1}$ and $d_i = 1$. This time evolution has a steady state that is reached in the following manner: $s(x,t)$ falls to $s \approx 0.04$, $i(x,t)$ falls immediately to $i = 0$ and $r(x,t)$ raises to $r \approx 0.96$, at about $t = 15$. Once the populations transition to a spatially inhomogeneous progression, their time evolution should follow the SIR model. This is indeed the case as seen in Fig 4.11, where the total populations $S(t)$, $I(t)$ and $R(t)$ of the diffusive SIR model have good agreement with the total populations of the SIR model. Although there is good agreement between the models, there is a very small yet definite, epidemic outbreak. If we recall from Chapter 2, an epidemic outbreak occurs when the value for $I(t) > I(0)$ for some $t$. This appears to be the case, but the behavior of the totals for the diffusive SIR model are essentially identical to the SIR-model as the values of the populations equilibrate as follows: $S(t)$ goes to $S = 0.04$ (4% susceptible population), $I(t)$ goes to $I = 0$ (no infected) and $R(t)$ goes to $R = 0.96$ (96% recovered population. Despite the qualitative difference represented by this almost insignificant epidemic outbreak, for strong diffusivities we can replace the integral of the products with the product of the integrals. However, for another regime in parameter space, the strength of the epidemic outbreak will be very significant.

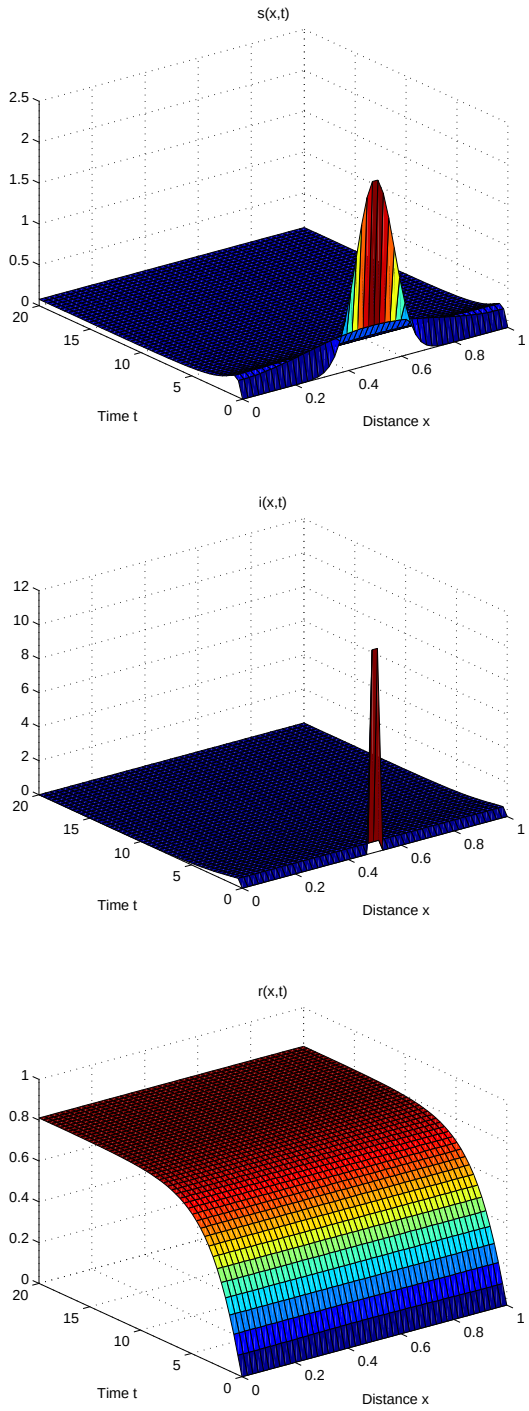


Figure 4.10: Solution of the Diffusive SIR model with $d_s = d_r = 1$ and $d_i = 0.1$ (regime I: strong SIR-diffusion). For the populations, $s(x,t)$, $i(x,t)$ and $r(x,t)$ become spatially homogeneous after a very short adjustment time.

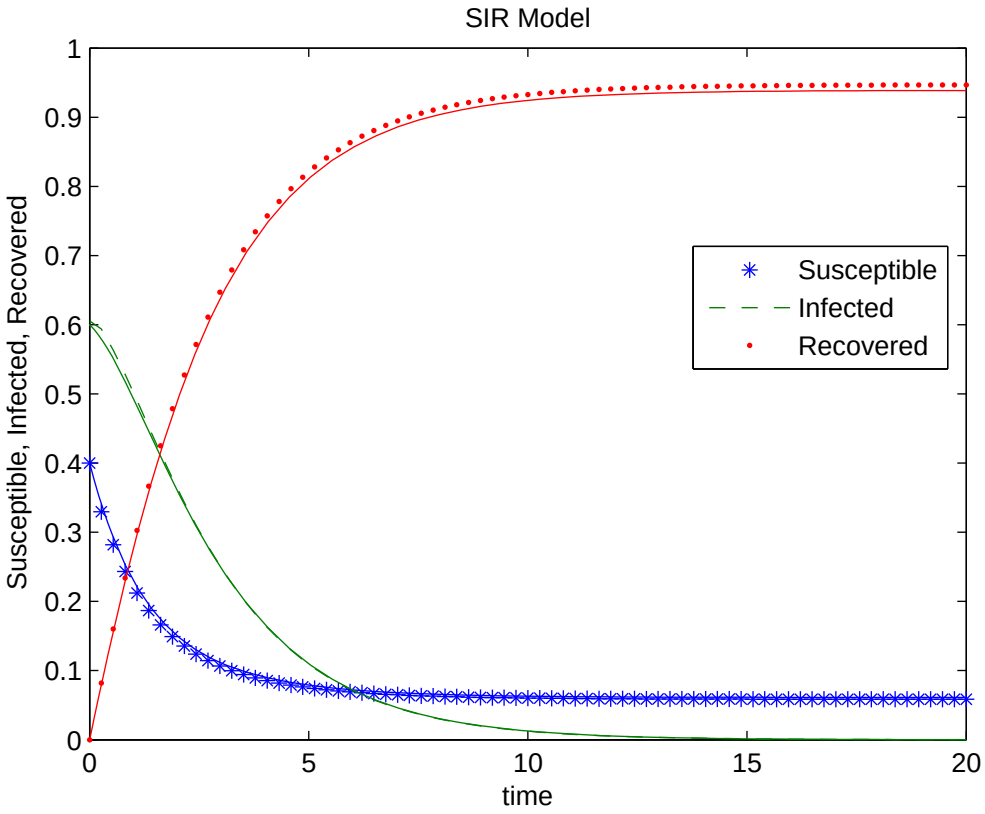


Figure 4.11: Comparison of the totals for the susceptible (S), infected (I) and recovered (R) individuals from the diffusive SIR epidemic system when $d_s = d_r = 1$ and $d_i = 0.1$ (strong SIR-diffusion regime) with the solution of the SIR model ($S_0 = 0.4$, $I_0 = 0.6$ and $R_0 = 0$). The solution of the diffusive SIR model equilibrates at the same rate.

## **Regime II:** (strong I-diffusion and weak SR-diffusion regime)

This regime corresponds to values $d_s = d_r \leq 10^{-2}$ and $d_i \geq 10^{-1}$ in the numerical experiments. It is characterized by the rapid homogenization of the infectives and the slow homogenization of the susceptibles and recovered. This is made clear in Fig 4.12 with $d_s = d_r = 10^{-3}$ and $d_i = 1$. Homogeneous final fate for all populations with $s(x,t)$ going to $s \approx 0.04$, $i(x,t)$ appears to increase slightly to a maximum value then decreasing to $i = 0$ and $r(x,t)$ increases to $r \approx 0.96$ at time $t = 15$. This epidemic development is similar to the development seen in the previous regime and therefore we should expect a small increase to infected population implying the presence of a small epidemic outbreak. In Fig 4.13, we see that indeed this is the case for the comparison of the total populations $S(t)$, $I(t)$ and $R(t)$ for the diffusive SIR model and their counterparts for the SIR model. We see a slight increase to the initial infected population and as before, the time evolution of total populations for the diffusive SIR models mirrors that of the SIR model for diffusivities $d_s = d_r = 10^{-3}$ and $d_i = 1$. Obviously we have good agreement between the two models, with equilibration time occurring at time $t = 15$. Again in this case we can replace the diffusive SIR model by the simpler SIR model.

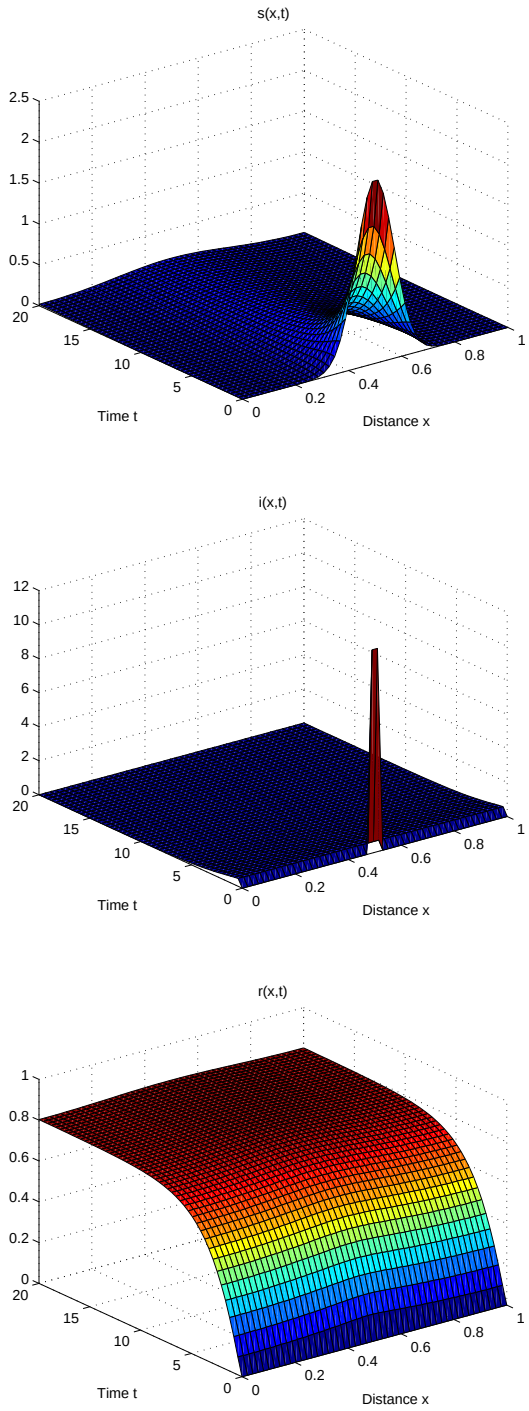


Figure 4.12: Solution of the Diffusive SIR model with $d_s = d_r = 0.001$ and $d_i = 1$ (regime II: strong I-diffusion and weak SR-diffusion). For the populations, $s(x,t)$ and $r(x,t)$ show spatial inhomogeneity until equilibrium is reached, $i(x,t)$ becomes spatially homogeneous after a very short adjustment time.

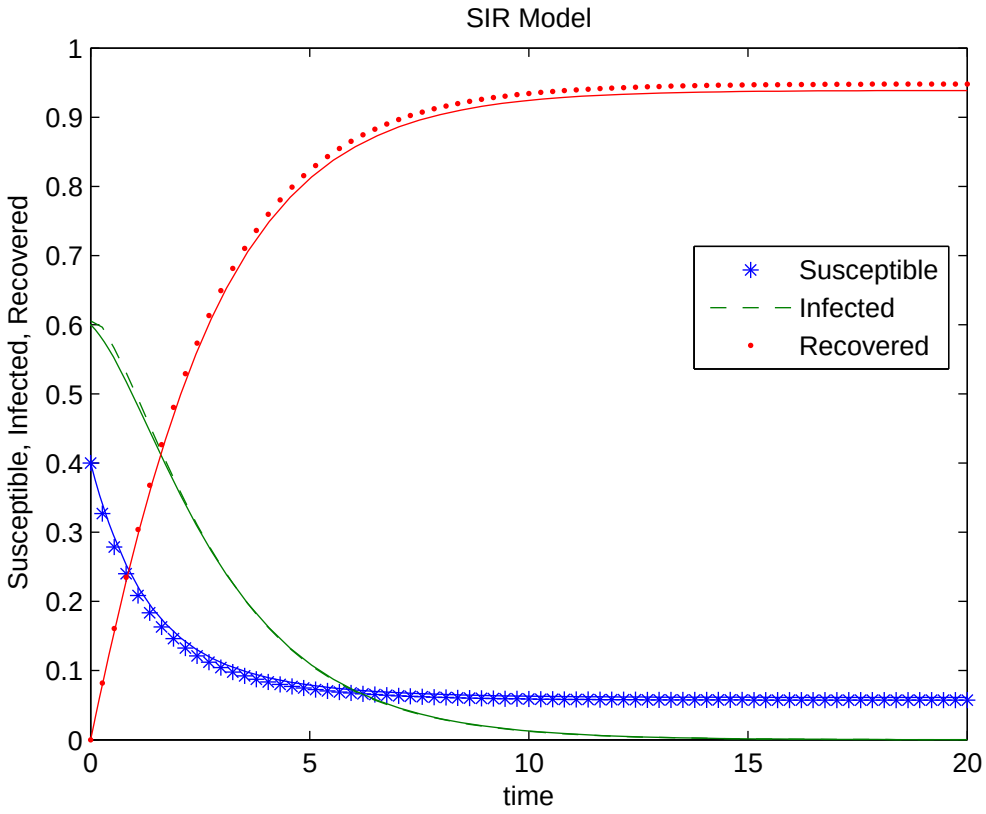


Figure 4.13: Comparison of the totals for the susceptible (S), infected (I) and recovered (R) individuals from the diffusive SIR epidemic system when $d_s = d_r = 0.001$ and $d_i = 1$ (strong I-diffusion and weak SR-diffusion regime) with the solution of the SIR model ($S_0 = 0.4$, $I_0 = 0.6$ and $R_0 = 0$). The solution of the diffusive SIR model equilibrates at the same rate.

## **Regime III:** (weak I-diffusion and strong SR-diffusion regime)

This regime corresponds to values $d_s = d_r \geq 10^{-1}$ and $d_i \leq 10^{-3}$ in the numerical experiments. It is characterized by the rapid homogenization of the susceptible and recovered individuals and the slow homogenization of the infectives. This is made clear in Fig 4.14 with $d_s = d_r = 1$ and $d_i = 10^{-3}$. Eventually all populations become constant in space with $s(x,t)$ going to $s \approx 0.04$, $i(x,t)$ appears to increase by a small amount to a maximum value then decreasing to $i = 0$ and $r(x,t)$ increases to $r \approx 0.96$. This apparent small increase to the infected population implies a mild epidemic outbreak. If this is the case then we should once again have for the total population of the infectives $I(t)$ a $T_* > 0$ so that $I(t) > I_0$ for $0 \leq t \leq T_*$ and thus an epidemic outbreak. In Fig 4.15, we see this is correct for the comparison of the total populations $S(t)$, $I(t)$ and $R(t)$ for the diffusive SIR model and their counterparts for the SIR model. We have the diffusive SIR model predicting epidemic outbreak and no epidemic outbreak predicted for the SIR-model. Once more we have good agreement between the two models. In general, this agreement deteriorates as $d_s$, $d_r$ decreases and the magnitude of the epidemic gets more pronounced.

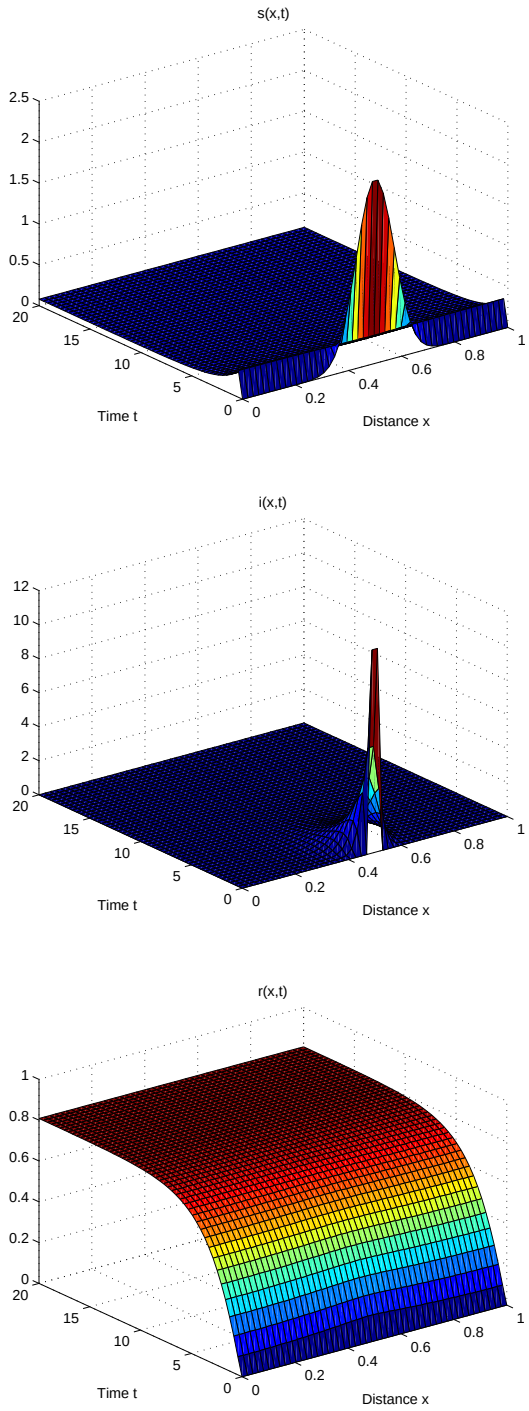


Figure 4.14: Solution of the Diffusive SIR model with $d_s = d_r = 1$ and $d_i = 0.001$ (regime III: weak I-diffusion and strong SR-diffusion). For the populations, $s(x,t)$ and $r(x,t)$ become spatially homogeneous after a very short adjustment time and $i(x,t)$ shows spatial inhomogeneity until equilibrium is reached.

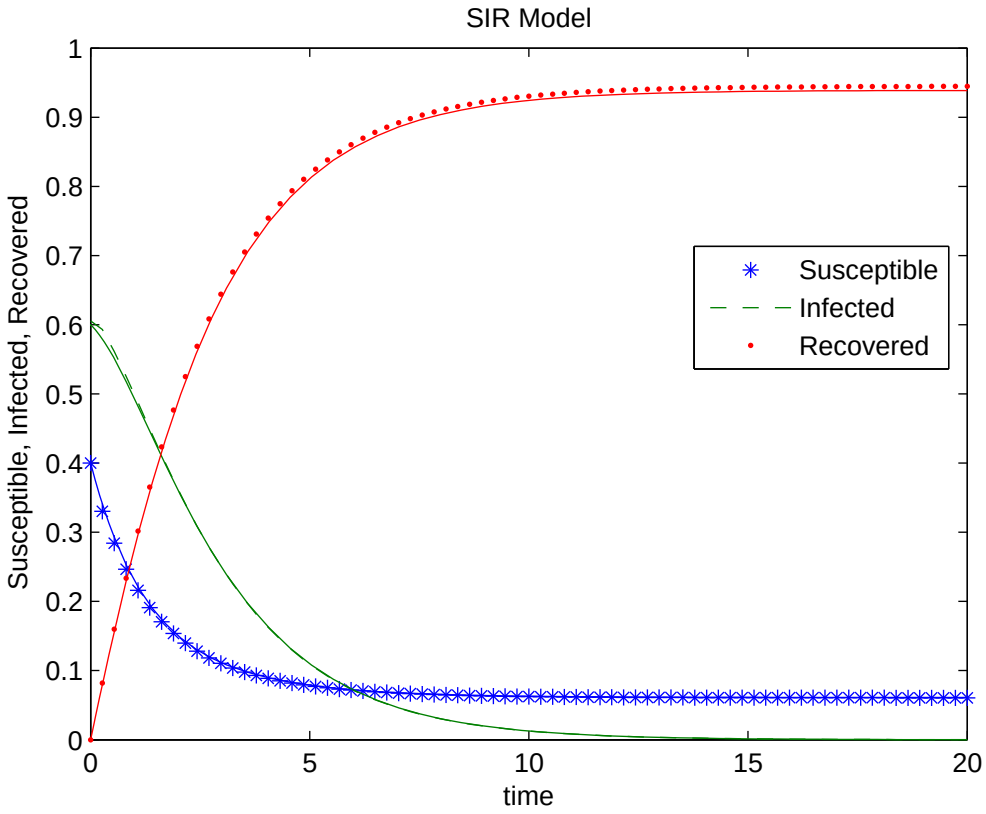


Figure 4.15: Comparison of the totals for the susceptible (S), infected (I) and recovered (R) individuals from the diffusive SIR epidemic system when $d_s = d_r = 1$ and $d_i = 0.001$ (weak I-diffusion and strong SR-diffusion regime) with the solution of the SIR model ($S_0 = 0.4$, $I_0 = 0.6$ and $R_0 = 0$). The solution of the diffusive SIR model equilibrates at the same rate.

## **Regime IV:** (weak SIR-diffusion regime)

This regime corresponds to values $d_s = d_r \leq 10^{-2}$ and $d_i \leq 10^{-1}$ in the numerical experiments. It is characterized by the slow homogenization of all species. Also, there is a persistence of spatial structure for the recovered population. This is obvious in Fig 4.14 with $d_s = d_r = 10^{-3}$ and $d_i = 10^{-2}$. Eventually we have a homogeneous steady state for all populations with $s(x,t)$ going to $s \approx 0.01$, $i(x,t)$ appears to increase by a small amount to a maximum value then decreasing to $i = 0$ and $r(x,t)$ increases to $r \approx 0.99$ at time $t = 15$. The increase to the infected population yields a pronounced epidemic outbreak in this regime. In Fig 4.15, we see that this is true for the comparison of the total populations $S(t)$, $I(t)$ and $R(t)$ for the diffusive SIR model and their counterparts for the SIR model. For the total values, $S(t)$ goes to $S = 0.01$ (1% susceptible population), $I(t)$ goes to $I = 0$ (no infected) and $R(t)$ goes to $R = 0.99$ (99% recovered population) at time $t = 4$ for $d_s = d_r = 10^{-3}$ and $d_i = 10^{-2}$. Obviously we do not have good agreement between the two models. The diffusive SIR model predicts epidemic outbreak of significant magnitude. In general, discrepancies between the diffusive SIR model and the SIR-model as $d_s$, $d_i$ and $d_i$ approach zero. Discrepancy becomes less as $d_s$, $d_r$ increase with $d_i$ fixed. Oddly enough, the highest epidemic outbreak does not occur when $d_s, d_r = 0$, $d_i = 0$ but rather when $d_s, d_r = 10^{-3}$, $d_i = 10^{-2}$. Clearly replacing the diffusive SIR with the SIR-model is no longer acceptable in this regime.

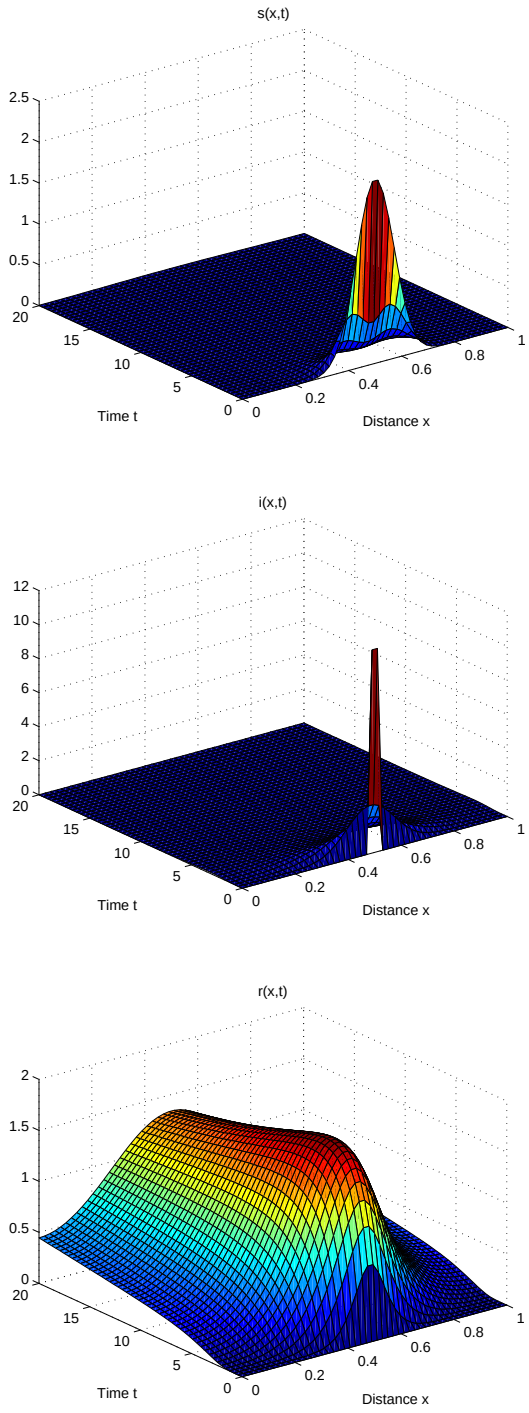


Figure 4.16: Solution of the Diffusive SIR model with $d_s = d_r = 0.001$ and $d_i = 0.01$ (regime III: weak SIR-diffusion). For the populations, $s(x,t)$, $i(x,t)$ and $r(x,t)$ show spatial inhomogeneities until the equilibrium time.

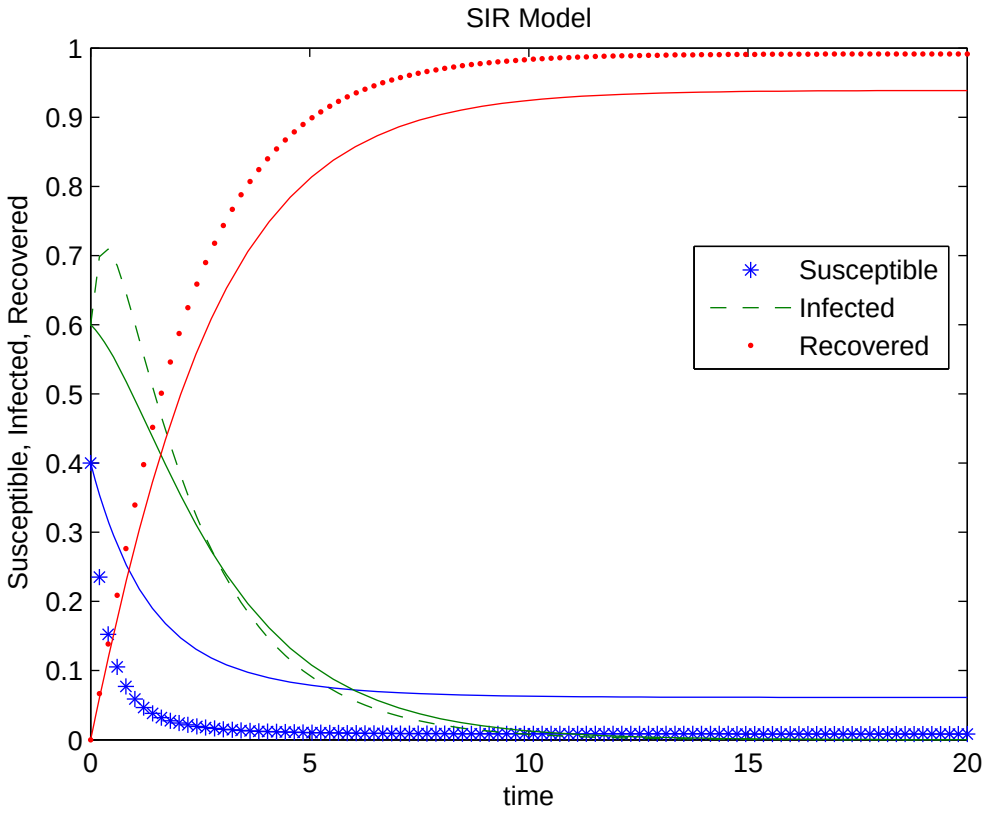


Figure 4.17: Comparison of the totals for the susceptible (S), infected (I) and recovered (R) individuals from the diffusive SIR epidemic system when $d_s = d_r = 0.001$ and $d_i = 0.01$ (weak SIR-diffusion regime) with the solution of the SIR model ($S_0 = 0.4$, $I_0 = 0.6$ and $R_0 = 0$). The solution of the diffusive SIR model equilibrates at a faster rate.

# Chapter 5

# Conclusion

In this thesis we carried out a systematic study and comparison of four basic models utilized in the theory of epidemics. These models are the SI and SIR models and the diffusive SI and SIR models. If we recall, the latter models include spatial displacements, in the form of simple diffusion for the individuals that occupy a specified area, which is the main distinction between the non-diffusive and diffusive models. Now, our goal with this paper was to chronicle each models characteristics and qualitative behavior and then compare them with their counterpart model, that is, the SI model with the diffusive SI model and the SIR model with the diffusive SIR model, where we dictated that the diffusion essentially be the difference. We did this in order to establish whether the diffusion or movements of the individuals would affect how the potential epidemics developed. This included the possibility of slower or faster times for a steady state to reached, and the existence or non-existence of an epidemic within one model and not the other, where we could conclude that indeed the spatial displacements did have an impact or we could have no obvious divergence between the models and in this case we could say that the added diffusion had no impact.

In Chapter 2 we looked at the SI and SIR models, first giving the background information and setting up these models, then giving detailed accounts of how epidemics did or did not develop and the nature by which they did within them. For the SI model, epidemic development is brought about simply by the existence of infected individuals, not a specified amount, but merely greater than zero. For the SIR model, epidemic development is predicated on a critical parameter $c$ such that if the total number of susceptibles is above or below this parameter, than we either have epidemic growth or hindrance respectively. These conditions for epidemic development are important, not only to this model but also to the diffusive models previously mentioned, seeing as we apply them to these models.

In Chapter 3 we looked at the diffusive SI model for equal and non-equal diffusivities. We once again detailed the behavior of the individuals by means of numerical solutions. We categorized the unique solutions and then detailed their characteristics. We then compared the SI model with the diffusive SI model by looking at the total populations for both models. We superimposed the plots of the total values of each individual for both models on top of one another which allowed for an easy comparison. For certain diffusivity values we saw marked changes, notably, steady states being reached at later times for the diffusive SI model and for other diffusivities we saw no changes. For strong infective diffusivity, we had good agreement between the diffusive SI model and the SI model, regardless of the susceptible diffusivity. For weak susceptible and infected diffusivity we had poor agreement between the two models.

In Chapter 4 we looked at the diffusive SIR model for equal and non-equal diffusivities and for the supercritical and subcritical cases $s_0 > c$ and $s_0 < c$ respectively. We categorized the unique solutions in various regimes according to the strength of the diffusivities and detailed their features both qualitatively and quantitatively. Next we compared predictions for the totals of the different populations for both

the SIR model and the diffusive SIR model. This brought about the following scenarios for the models: epidemic outbreak for both for the supercritical case. We also saw that for the subcritical case, the SIR model predicts no epidemic outbreak whereas the diffusive SIR model always predicts an outbreak, even though it may be quite small unless the diffusivities are weak. Granted, this scenario occurs with the Neumann boundary conditions, but this may not be the case, with Dirichlet boundary conditions, which allow for the declining of the individuals, that is, the total population does not remain constant and eventually would go to zero as time increased.

For the supercritical case we conclude that regardless of $d_i$, if $d_s = d_r$ is strong then good agreement between the diffusive SIR model and the SIR model is present. If $d_s = d_r$ is weak, poor agreement between the models, in spite of the fact that the initial distribution of $S$ and $R$ are broadly spread in relation to $I$. For the subcritical case we conclude that for weak diffusivities, $d_s$, $d_i$ and $d_r$, we have a significant epidemic outbreak for the diffusive SIR model, in contrast with the SIR-model which displays no epidemic outbreak in the subcritical case. Needless to say, the agreement in the predictions of the two models in their subcritical regime with weak diffusivites is rather poor.

Finally we say, that in certain instances, the SI and SIR models and the diffusive SI and SIR models, with all things equal apart from the diffusion, diverge quite significantly. Therefore we can say that the introduction of individuals movements or diffusion can have a significant impact on epidemic development.

# References


[1] Anderson, R.M., Jackson, H.C., May, R.M, Smoth, A.M., "Population dynamics of fox rabies in Europe", Nature 289, 765-771, 1981

[2] Anderson, R.M., May, R.M., Infectious Diseases of Humans. Dynamics and Control, Oxford University Press, Oxford, 1991

[3] Anderson, R.M., Medley, G.F., May, R.M., Johnson, A.M, "A Preliminary study of the transmission dynamics of the human immunodeficiency virus (HIV), the causitive agent of AIDS. IMA J. Maths. Appl. in Medicure and Biology 3, 229-263, 1986

[4] Bernoulli, D., "Essai ́dune nouvelle analyse de la mortalité causeé par la petite vé et des avantages de ́linoculation pour la prevéruir". Histoire de ÍAcad. Roy. Sci. (Paris) avec Méiu des Math. et Phys., 1-45, 1760

[5] Edelstein-Keshet, L.V., Mathematical Models in Biology, Random House, New York, 1988

[6] Fife, P.C., Mathematical Aspects of Reacting and Diffusing Systems. Lecture Notes in Biomathematics.28, Springer, New York, 1979

[7] Fisher, R.A., "The wave of advance of advantageous genes", Ann. Eugenics, 7, 353-369, 1937

[8] Hethcote, M.W., Yorke, J.A., Gonorrhea Transmission Dynamics and Control, Lecture Notes in Biomathematics. 56, Springer, New York, 1984

[9] Highman, D., Highman, N., Matlab Guide, SIAM, Philadelphia, PA, 2000

[10] Hoppensteadt, F.C., Mathematical Theories of Population: Demographics, Genetics and Epidemics. CBMS Lectures Vol. 20. SIAM Publications, Philadelphia, PA, 1975

[11] Hoppensteadt, F.C., Mathematical Methods in Population Biology, Cambridge University Press, Cambridge, 1982

[12] Källén, A., Arcari, P., Murray, J.D., "A simple model for the spatial spread and control rabies", J. Theor. Biol. 116, 377-393, 1985

[13] Keeling, M.J., Rohani, P., Modeling Infectious Diseases in Humans and Animals, Princeton University Press, NJ, USA, 2008

[14] Kermack, W. O. and McKendrick, A. G. "A Contribution to the Mathematical Theory of Epidemics." Proc. Roy. Soc. Lond. A 115, 700-721, 1927

[15] Kermack, W. O. and McKendrick, A. G. "A Contribution to the Mathematical Theory of Epidemics." Proc. Roy. Soc. Lond. A 138, 55-83, 1932

[16] Kermack, W. O. and McKendrick, A. G. "A Contribution to the Mathematical Theory of Epidemics." Proc. Roy. Soc. Lond. A 141, 94-122, 1933

[17] Kolmogoroff, A., Petrovsky, I., Piscounoff, N., "Étude de Iéquation de la diffusion avec croissance de la quantité de matiére et son application á un probléme biologigue", Moscow Univ. Bull. Math.1, 1-25, 1937

[18] MacDonald, D.W., Rabies and Wildlife: a biologists perspective, Oxford University Press, Oxford, 1980

[19] Murray, J.D. Mathematical Biology, I: An Introduction, 3rd edition, Springer-Verlag Berlin Heidelberg, 2003

[20] Murray, J.D. Mathematical Biology, II: Spatial Models and Biomedical Applications, 3rd edition, Springer-Verlag Berlin Heidelberg, 2003

[21] Murray, J.D., Stanley, E.A., Brown, D.L, "On the spatial spread of rabies among foxes", Proc. Roy. Soc. (London) B229, 111-150, 1986

[22] Murray, J.D., Seward, W.L., "On the spatial spread of rabies among foxes with immunity", J. Theor. Biol., 156:327-346, 1992

[23] Noble, J.V., "Geographic and temporal development of plague", Nature 250, 326-728, 1974

[24] Raggett, G.F., "Modelling the Eyam Plague", Bull. Inst. Math and its Application 18, 221-226, 1982

[25] Verhulst, P.F. "Notice sur la loi que la poulation suit dans son accroissement", Corr. Math. et Phys. 10, 113-121, 1838